PHYSICAL REVIEW D **78,** 055016 (2008)

Triplet extended supersymmetric standard model

Stefano Di Chiara* and Ken Hsieh+

Department of Physics, Michigan State University, East Lansing, Michigan 48824, USA

(Received 1 June 2008; revised manuscript received 29 July 2008; published 22 September 2008)

We revisit an extension of the minimal supersymmetric standard model (MSSM) by adding a hypercharge-neutral, $SU(2)$-triplet chiral superfield. Similar to the next-to-minimal supersymmetric standard model , the triplet gives an additional contribution to the quartic coupling in the Higgs potential, and the mass of the lightest CP-even Higgs boson can be greater than M_Z at tree level. In addition to discussing the perturbativity, fine-tuning, and decoupling issues of this model, we compute the dominant 1-loop corrections to the mass of the lightest CP-even Higgs boson from the triplet sector. When the Higgs-Higgs-Triplet coupling in the superpotential is comparable to the top Yukawa coupling, we find that the Higgs mass can be as heavy as 140 GeV even without the traditional contributions from the top–s-top sector, and at the same time consistent with the precision electroweak constraints. At the expense of having Landau poles before the grand unified theory scale, this opens up a previously forbidden region in the MSSM parameter space where both s-tops are light. In addition to having relatively small fine-tuning (about one part in 30), this leads to a gluophilic Higgs boson whose production via gluon-gluon fusion at the CERN LHC can be twice as large as the standard model prediction.

DOI: 10.1103/PhysRevD.78.055016 PACS numbers: 12.60.Jv, 12.60.Cn, 14.80.Cp, 14.80.Ly

I. INTRODUCTION

The electroweak sector of the standard model (SM) predicts new physics at sub-TeV scales to unitarize WW scattering. With a Higgs boson, the hierarchy problem suggests additional new physics near the TeV scale to stabilize the electroweak scale, and the minimal supersymmetric standard model (MSSM) is one of the leading candidates of such new physics. For reviews of the MSSM, see, for example, Drees [1], Martin [2], Dine [3], and Peskin [4].

In the MSSM, the mass of the lightest CP-even Higgs boson is bounded at tree level by M_Z because the tree-level quartic couplings are parameterized by gauge couplings, and such a light Higgs boson is ruled out by the CERN LEP searches of the SM Higgs boson [5–9] that impose

$$m_h^{\mathrm{SM}} > 114.4 \text{ GeV}. \tag{1}$$

At one-loop level, however, there can be large radiative corrections due to heavy scalar tops ($\tilde{Q}_3$ and $\tilde{U}_3$, superpartners of the top quark) and/or a large coupling of the trilinear interaction $\tilde{Q}_3 H_u \tilde{U}_3$ [10–19]. While such radiative corrections can be large enough to satisfy the LEP bounds, they also contribute to the quadratic term of the Higgs potential, leading to the ''little hierarchy problem.'' The MSSM also suffers from a μ problem in that its lone dimensionful SUSY-invariant parameter, μ, is phenomenologically required to be of order 100 GeV, while its natural scale can in principle be much larger.

The next-to-minimal supersymmetric standard model (NMSSM) solves the μ problem and alleviates the little hierarchy problem [20] by extending the MSSM with a singlet chiral superfield S. For reviews of the NMSSM, see Balazs *et al.* [21] and references therein. The Higgs couplings with S lead to additional contributions to the quartic couplings in the Higgs potential, while the μ term is dynamically generated from the vacuum expectation value (vev) of the scalar component of S. With these additional contributions to the quartic couplings, the mass of the lightest CP-even Higgs boson may be larger than M_Z at tree level, and the NMSSM can satisfy the LEP bounds on the Higgs mass with lighter s-tops compared to the MSSM [22–28].

In this paper, we extend the MSSM with a hypercharge-neutral, $SU(2)$-triplet chiral superfield T and name the model triplet-extended supersymmetric standard model (TESSM). Extensions of this type have been studied extensively by Espinosa and Quiros [29,30], Felix-Beltran [31], Setzer and Spinner [32], and Diaz-Cruz *et al.* [33]. While this model does not solve the μ problem, it is an interesting alternative to the NMSSM, as an economical extension of the MSSM, because it can also achieve a mass of the lightest CP-even Higgs boson that is larger than M_Z at tree level. Furthermore, compared to the MSSM and the NMSSM, we expect there to be more radiative corrections to the mass of the lightest CP-even Higgs boson due to the additional states in the triplet. To the extent that these triplet-induced radiative corrections are significant, we may further alleviate the little hierarchy problem.

Unfortunately, in both the NMSSM and the TESSM, the respective singlet-induced and triplet-induced radiative corrections are typically small when we demand perturbativity at the scale of grand unified theory (GUT) near 10^{16} GeV. This is because perturbativity at the GUT scale imposes the bound $\lambda \lesssim 0.7$ at the weak scale, where λ

*dichiara@msu.edu
+kenhsieh@pa.msu.edu

is, respectively, the Higgs-singlet-Higgs and the Higgs-triplet-Higgs coupling in the superpotential of the NMSSM and TESSM. In both models, while the tree-level mass of the lightest CP-even Higgs boson can be as large as 100 GeV, the $\mathcal{O}(\lambda^4)$ radiative corrections are not large enough to lift the Higgs mass over the LEP bounds. On the other hand, in the TESSM, when we have $\lambda \sim 0.9$ (so that λ is comparable with the top Yukawa coupling) at the weak scale, we find the tree-level mass of the lightest CP-even Higgs boson to be close to the LEP bound and the $\mathcal{O}(\lambda^4)$ radiative corrections alone can easily lift the Higgs mass over the LEP bound even with small SUSY breaking in the triplet sector. As the small SUSY breaking in the triplet sector translate into small fine-tuning, we can solve the little hierarchy problem at the expense of giving up perturbativity at the GUT scale.

Without demanding perturbativity at the GUT scale, we also expect the NMSSM to be a solution to the little hierarchy problem, with the mass of the lightest CP-even Higgs boson that satisfies the LEP bounds without significant contribution from the top–s-top sector. However, as an alternative to the NMSSM and a reasonably economical extension of the MSSM, the TESSM and its phenomenology are interesting in their own right. For example, as we show in this paper, the MSSM limit of the TESSM is achieved with $M_T \to \infty$, where M_T is the SUSY-invariant mass of the triplet, keeping λ fixed, whereas in the NMSSM one requires $\lambda \to 0$ to achieve the MSSM limit. As another example, even though the sub-TeV, electrically-neutral component of the triplet acquires a vev, we can still satisfy the precision electroweak constraints without the extreme fine-tuning noted in the triplet-extended SM [34]. Moreover, there may be other considerations that motivate extending the MSSM by a triplet instead of a singlet. For example, in obtaining neutrino masses through the type-II [35] and type-III seesaw mechanisms, the SM is commonly extended with Higgs triplets. Though the Higgs triplets may have nonzero hypercharge, hypercharge-neutral triplets are often present when the models are supersymmetrized and embedded in a unified gauge group [32,36,37].

We organize our paper as follows. In Sec. II, we lay out the superpotential and the Lagrangian of the TESSM, compare it to the NMSSM, and discuss constraints on its parameter space from electroweak precision tests and the requirement of perturbativity at the GUT scale. In Sec. III, we numerically evaluate the mass of the lightest, CP-even Higgs boson to one loop, and show that we can satisfy the LEP2 bounds without the contributions from the top–s-top sector when λ is comparable with the top Yukawa coupling. We also discuss the gluon-gluon fusion production and diphoton decay of the lightest, CP-even Higgs boson in Sec. III. Our discussions of the gluon-gluon fusion production rely only on the existence of light s-tops and the minimal color sector of the MSSM, and are therefore applicable to any extensions of the MSSM that solves the little hierarchy problem without invoking additional colored states. In Sec. IV, we estimate two sources of fine-tuning in this model, and find that we can achieve a small fine-tuning of about one part in 30 in the Higgs sector. Finally, we conclude with Sec. V that summarizes our results.

II. TRIPLET-EXTENDED SUPERSYMMETRIC STANDARD MODEL

A. The model

We extend the MSSM with a hypercharge-neutral, $SU(2)$ triplet $T \equiv \frac{1}{2}\sigma^A T^A$ with the superpotential

$$W_{\text{TESSM}} = \mu H_d H_u + M_T \,\text{Tr}(TT) + 2\lambda H_d T H_u + \alpha_T \,\text{Tr}(T) + W_{\text{Yukawa}}, \tag{2}$$

where $H_{u,d}$ are the Higgs doublets of the MSSM, α_T is a Lagrange multiplier determined from the potential, and W_{Yukawa} is the MSSM superpotential sans the μ term

$$W_{\text{Yukawa}} = y_t Q H_u U^c + y_b Q H_d D^c + y_\tau L H_d E^c. \tag{3}$$

Note that, since T is a chiral superfield, its scalar component necessarily contains a *complex* $SU(2)$ triplet, whereas in non-SUSY extensions of the SM [34,38–42], we can extend the SM with a real $SU(2)$ triplet. In components, we have the fields

$$H_u = \begin{pmatrix} H_u^+ \\ H_u^0 \end{pmatrix}, \qquad H_d = \begin{pmatrix} H_d^0 \\ H_d^- \end{pmatrix}, \qquad T = \frac{1}{2}\begin{pmatrix} T^0 & \sqrt{2}T^+ \\ \sqrt{2}T^- & -T^0 \end{pmatrix}, \tag{4}$$

and the superpotential (sans the SM Yukawa couplings)

$$W_{\text{TESSM}} \supset \mu(H_u^+ H_d^- - H_u^0 H_d^0) + \frac{M_T}{2}(T^0 T^0 + 2T^+ T^-) + \lambda(H_d^0 T^0 H_u^0 + H_d^- T^0 H_u^+) + \sqrt{2}\lambda(H_d^- T^+ H_u^0 - H_d^0 T^- H_u^+). \tag{5}$$

The factor of 2 in front of λ in Eq. (2) gives us a coefficient of unity for the term

$$W_{\text{TESSM}} \supset \lambda H_d^0 T^0 H_u^0, \tag{6}$$

as with the case of the NMSSM when T^0 is replaced by a singlet S, and facilitates direct comparisons between TESSM and NMSSM.

We can achieve gauge coupling unification at M_{GUT} by including additional chiral superfields with quantum numbers

$$D \sim (\mathbf{1}, \mathbf{2})_{1/2}, \qquad \bar{D} \sim (\mathbf{1}, \mathbf{2})_{-1/2}, \qquad G \sim (\mathbf{8}, \mathbf{1})_0, \tag{7}$$

where the first and second entries inside the parenthesis denote, respectively, the representations under the color $SU(3)_c$ and weak $SU(2)_w$ gauge groups, and the subscripts denote the charge under hypercharge $U(1)_Y$ gauge group.

This added content can have both SUSY-invariant and SUSY-breaking masses sufficiently large (say, 2 TeV) so that they decouple from the electroweak scale physics, while still allowing for gauge coupling unification. The added matter content [triplet plus those in Eq. (7)] does not constitute a complete multiplet of $SU(5)$, but can form a complete multiplet of trinification group $SU(3)^3 \times Z_3$ [43–45].

In addition to the MSSM soft SUSY-breaking parameters, we also have soft terms involving T

$$-\Delta\mathcal{L} = 2m_T^2\,\mathrm{Tr}(T^\dagger T) + B_T(\mathrm{Tr}(TT) + \mathrm{H.c.}) + 2\lambda A_\lambda(H_d T H_u + \mathrm{H.c.}). \quad (8)$$

B. Comparison to the NMSSM

1. Perturbativity

For simplicity, we assume that all couplings and masses in the superpotential are real. The tree-level potential involving the $U(1)_{\mathrm{em}}$-neutral Higgs doublets and triplet is then

$$V_{\mathrm{TESSM}} = V_H + V_T + V_{\mathrm{mix}}, \quad (9)$$

where

$$V_H = (\mu^2 + m_{H_u}^2)|H_u^0|^2 + (\mu^2 + m_{H_d}^2)|H_d^0|^2 - B_\mu(H_u^0 H_d^0 + \mathrm{c.c.}) + \tfrac{1}{8}(g_2^2 + g_1^2)(|H_u^0|^2 - |H_d^0|^2)^2 + \lambda^2|H_u^0|^2|H_d^0|^2, \quad (10)$$

$$V_T = (M_T^2 + m_T^2)|T^0|^2 + \frac{B_T}{2}(T^0T^0 + \mathrm{c.c.}), \quad (11)$$

$$V_{\mathrm{mix}} = \lambda^2|T^0|^2(|H_u^0|^2 + |H_d^0|^2) + \lambda M_T(H_d^0 T^{0*} H_u^0 + \mathrm{c.c.}) + \lambda A_\lambda(H_d^0 T^0 H_u^0 + \mathrm{c.c.}) - \lambda\mu(H_u^{0*} T^0 H_u^0 + H_d^{0*} T^0 H_d^0 + \mathrm{c.c.}). \quad (12)$$

Compared with the Higgs potential in the MSSM, we have an enhancement in the quartic coupling of the form

$$V \supset \lambda^2|H_u|^2|H_d|^2, \quad (13)$$

and this in principle allows for a tree-level mass eigenvalue larger than M_Z after electroweak symmetry breaking (EWSB). This is similar to the case in the NMSSM, where such quartic couplings are also generated from a superpotential of the form

$$W_{\mathrm{NMSSM}} = \lambda S H_d H_u + \frac{\kappa}{3}S^3. \quad (14)$$

As with the NMSSM, where the requirement of perturbativity at the GUT scale limits $\lambda \lesssim 0.7$ at the TeV scale, the TESSM also has a bound $\lambda \lesssim 0.7$ at the TeV scale while still preserving perturbativity at the GUT scale. Though the bounds are similar, the details of obtaining such bounds are different and may be important for further model building where perturbativity at the GUT scale is imposed. We elaborate briefly on some key differences between the two models from the relevant renormalization group equations (RGEs) given by

$$\beta_\lambda^{\mathrm{TESSM}} = \frac{\lambda}{16\pi^2}(8\lambda^2 + 3y_t^2 - 9g_2^2 - g_1^2), \quad (15)$$

$$\beta_\lambda^{\mathrm{NMSSM}} = \frac{\lambda}{16\pi^2}(4\lambda^2 + 2\kappa^2 + 3y_t^2 - 3g_2^2 - g_1^2), \quad (16)$$

$$\beta_\kappa^{\mathrm{NMSSM}} = \frac{\kappa}{16\pi^2}(6\lambda^2 + 6\kappa^2), \quad (17)$$

and note the following points:

(i) In the NMSSM, there are two possible Landau poles in λ and κ. The RGE of κ is such that κ always increases when evolving to higher energies, and κ feeds into the evolution of λ. In the TESSM, there is no such contribution because $\mathrm{Tr}(T^3) = 0$, but there are now additional contributions to the λ^3 coefficient in β_λ in the TESSM.

(ii) In the TESSM, β_λ has a larger coefficient for the negative contribution of the form λg_2^2 because T is charged under $SU(2)$. As the coupling g_2 is non-asymptotically-free in the TESSM (also in the NMSSM), this gives a stronger suppression at higher energies and could potentially delay the appearance of the λ Landau pole.

(iii) The coupling g_2 also flows to larger values in the TESSM than in the NMSSM because of the added matter content. This again gives a suppression at higher energies and may delay the λ Landau pole. (This can be achieved in the NMSSM with added matter content, for example, in the NMSSM with gauge-mediated SUSY breaking.)

Thorough studies on the upper bounds of λ in TESSM and its extensions would require examining fixed points from the RGEs, and we leave these investigations for the future. For our work, it suffices to note that perturbativity at the GUT scale imposes $\lambda \lesssim 0.7$ at the weak scale, so that λ is of similar strength to the weak gauge coupling. As such, while the tree-level mass of the lightest CP-even Higgs boson can be 100 GeV (as we later show), we expect the $\mathcal{O}(\lambda^4)$ radiative corrections to the mass of the lightest CP-even Higgs boson to be insufficient to lift the Higgs mass above the LEP bounds. However, motivated by solving the hierarchy problem, we take the viewpoint that the Landau pole we encounter at a higher scale (around 10^{10} GeV) is rescued by some other new physics and analyze the Higgs spectra and the phenomenology for larger values of λ. We take values of λ comparable to the top Yukawa coupling, so that the TeV-scale physics is still perturbative. As λ is now near unity at the TeV scale in the TESSM and we expect there to be more $\mathcal{O}(\lambda^4)$ radiative corrections to the mass of the lightest CP-even Higgs

boson compared to the NMSSM, it is worthwhile to investigate these radiative corrections in detail.

In extensions of the NMSSM, such as fat Higgs models [46–49], λ can achieve much larger values and give rise to a very large mass for the lightest CP-even Higgs boson. The model-building techniques of fat Higgs models can also be applied to the TESSM, but in this work we focus on the TESSM as a simple extension of the MSSM and an alternative to the NMSSM without imposing the constraint of perturbativity at the GUT scale.

2. The MSSM limit

In the NMSSM, the μ term and the masses of the singlet (ino) are related by

$$\mu \sim \lambda^{\mathrm{NMSSM}}\langle S\rangle, \qquad M_S \sim \kappa^{\mathrm{NMSSM}}\langle S\rangle, \tag{18}$$

and the MSSM limit is $M_S \to \infty$ while keeping μ fixed. Keeping κ perturbative in the MSSM limit then gives $\lambda \to 0$. As λ is the only coupling between the singlet and the MSSM sector, the MSSM limit of $\lambda \to 0$ with fixed μ decouples the singlet.

In the TESSM, the MSSM limit is achieved with $M_T \to \infty$, holding the values of all other masses and couplings at the weak scale fixed, and, in particular, we do not need $\lambda \to 0$ to achieve the MSSM limit. The decoupling of the additional contribution to the Higgs quartic coupling in Eq. (13) is accomplished by the effective operator obtained by integrating out the heavy triplet fields when $M_T \gg M_Z$. Setting $B_T = 0$ for simplicity, the equation of motion for T^0, among other terms, has contributions of the form

$$T^0 = -\frac{\lambda}{M_T^2 + m_T^2}(M_T H_d^0 H_u^0 + A_\lambda H_d^{0*} H_u^{0*} - \mu(H_u^{0*} H_u^0 + H_d^{0*} H_d^0)) + \cdots, \tag{19}$$

and this induces a contribution in the effective Lagrangian

$$-\Delta\mathcal{L}_{\mathrm{eff}} = -\lambda^2 \frac{M_T^2 + A_\lambda^2 + 2\mu^2}{M_T^2 + m_T^2}|H_d^0|^2|H_u^0|^2 + \cdots, \tag{20}$$

that cancels the λ^2 contribution to the quartic in the Higgs potential when $M_T^2 \gg A_\lambda^2, m_T^2, \mu^2$. In terms of Feynman diagrams, this effective operator arises from the diagrams such as the one shown in Fig. 1 with the amplitude (in the limit of large $M_T^2 \gg A_\lambda^2, m_T^2, \mu^2$)

$$i\mathcal{A} = \lambda^2 \frac{M_T^2}{p^2 - M_T^2}, \tag{21}$$

where $p \sim M_Z$ is the scale of external momenta of the Higgs bosons. In the limit $M_T^2 \gg p^2$, this gives the canceling contribution to the Higgs potential, and the resulting theory is the MSSM.

When we do not explicitly integrate out the heavy triplet sector, the full mass matrices (involving both Higgs doublets and the triplet) provide a seesawlike mechanism in the limit of $M_T \to \infty$ that seesaws away any λ dependence in the Higgs doublets sector. We will demonstrate this in the next section when we compute the mass of the lightest CP-even Higgs boson.

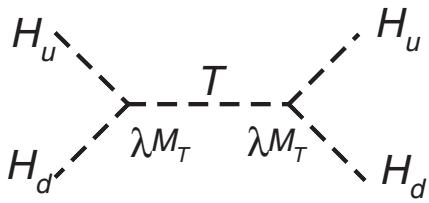

FIG. 1. An example of Feynman diagrams that give the contributions which cancel λ contributions in the Higgs potential when the triplet field, T, decouples.

C. EWSB in TESSM

As we are assuming real couplings and masses for simplicity, there is no mixing between the real and imaginary components of the complex scalar fields $H_{u,d}^0$ and T^0 and it is convenient to separate them into real and imaginary parts

$$H_u^0 = \frac{1}{\sqrt{2}}(a_u + \imath b_u) = \frac{1}{\sqrt{2}}(a_u' + \imath b_u) + \frac{1}{\sqrt{2}}v_u, \tag{22}$$

$$H_d^0 = \frac{1}{\sqrt{2}}(a_d + \imath b_d) = \frac{1}{\sqrt{2}}(a_d' + \imath b_d) + \frac{1}{\sqrt{2}}v_d, \tag{23}$$

$$T^0 = \frac{1}{\sqrt{2}}(a_t + \imath b_t) = \frac{1}{\sqrt{2}}(a_t' + \imath b_t) + \frac{1}{\sqrt{2}}v_t, \tag{24}$$

where we have also shifted the real components (a_i) to the physical modes (a_i') by the respective vacuum expectation values (v_i). Prior to EWSB, all the vevs vanish and the real components of the Higgses have the mass matrix (in the basis (a_u, a_d, a_t))

$$\mathcal{M}_a^2 = \begin{pmatrix} m_{H_u}^2 + \mu^2 & -B_\mu & 0 \\ -B_\mu & m_{H_d}^2 + \mu^2 & 0 \\ 0 & 0 & M_T^2 + m_T^2 + B_T \end{pmatrix}. \tag{25}$$

The corresponding mass matrix for the imaginary components can be obtained from Eq. (25) by changing the signs of B_T and B_μ in the (1,2), (2,1), and (3,3) elements.

In the MSSM, the conditions for successful EWSB breaking are that (i) the (top-left 2×2) mass matrix in Eq. (25) has one negative eigenvalue, and (ii) the potential is bounded from below along the D-flat direction $H_u^0 = H_d^0$. In the TESSM model, the first condition gives us the same condition as the MSSM

$$B_\mu^2 > (m_{H_u}^2 + \mu^2)(m_{H_d}^2 + \mu^2), \tag{26}$$

while the second condition is automatically satisfied by the presence of the quartic coupling $\lambda^2|H_d^0|^2|H_u^0|^2$. However, the minimization conditions now demand

$$v_t = \frac{\sqrt{2}}{2}(\lambda v^2)\frac{\mu - (A_\lambda + M_T)c_\beta s_\beta}{M_T^2 + m_T^2 + B_T + \frac{\lambda^2}{2}v^2}, \tag{27}$$

$$m_{H_u}^2 + \mu_{\rm eff}^2 = t_\beta^{-1}B_\mu + \frac{c_{2\beta}}{2}M_Z^2 - \frac{1}{2}\lambda^2 c_\beta^2 v^2 - \frac{\lambda v_t}{\sqrt{2}}(M_T + A_\lambda)t_\beta^{-1}, \tag{28}$$

$$m_{H_d}^2 + \mu_{\rm eff}^2 = t_\beta B_\mu - \frac{c_{2\beta}}{2}M_Z^2 - \frac{1}{2}\lambda^2 s_\beta^2 v^2 - \frac{\lambda v_t}{\sqrt{2}}(M_T + A_\lambda)t_\beta, \tag{29}$$

where we have defined

$$\mu_{\rm eff} \equiv \mu - \frac{1}{\sqrt{2}}\lambda v_t, \tag{30}$$

$$\tan\beta \equiv \frac{v_u}{v_d}, \qquad v^2 \equiv v_u^2 + v_d^2, \tag{31}$$

$$v_u = v\sin\beta, \qquad v_d = v\cos\beta, \tag{32}$$

so that the gauge bosons receive masses of

$$M_Z^2 = \tfrac{1}{4}(g_2^2 + g_1^2)v^2, \tag{33}$$

$$M_W^2 = \tfrac{1}{4}g_2^2 v^2 + g_2^2 v_t^2, \tag{34}$$

where g_2 and g_1 are, respectively, the gauge couplings of the $SU(2)$ and $U(1)_Y$ groups. We have also abbreviated for convenience the trigonometric functions

$$s_\beta \equiv \sin\beta, \qquad c_\beta \equiv \cos\beta, \qquad t_\beta \equiv \tan\beta, \qquad s_{2\beta} \equiv \sin 2\beta, \qquad c_{2\beta} \equiv \cos 2\beta. \tag{35}$$

D. Oblique corrections

While the condition of successful EWSB in Eq. (26) gives a constraint on the parameters, electroweak precision tests offer a much more stringent constraint. The induced vev v_t contributes to the oblique parameter αT because it contributes to the mass of the charged gauge bosons $W^\pm$, but not to that of the neutral gauge boson Z. We find the oblique contribution to be

$$\alpha\Delta T = \frac{\delta M_W^2}{M_W^2} = 4\frac{v_t^2}{v^2} = \frac{\lambda^2 v^2}{2}\left(\frac{2\mu - (A_\lambda + M_T)\sin 2\beta}{M_T^2 + m_T^2 + B_T + \frac{\lambda^2}{2}v^2}\right)^2. \tag{36}$$

The oblique correction due to the triplet vanishes in the limit of $M_T \to \infty$ holding all other parameters fixed, as expected. However, even if M_T is of the same order of μ and A_λ, ΔT can be small due to a partial cancellation between μ and $\sin 2\beta(A_\lambda + M_T)$.

We impose the constraint that $|\Delta T| < 0.1$, which in turn translates to an upper bound on v_t

$$|v_t| < 3.43 \text{ GeV},$$

and provides the main constraint on the parameters λ and M_T. In Fig. 2, we plot the allowed regions on $M_T - \lambda$ plane with $B_T = m_T^2 = A_\lambda^2 = (200 \text{ GeV})^2$, for various values of $\tan\beta$ and μ. For small values of $\tan\beta$ and μ, $\alpha\Delta T$ is only viable with either small λ or a cancellation in the numerator of Eq. (36). In Fig. 3, we plot the allowed region in $\mu - \tan\beta$ plane for $\lambda = 0.9$, $B_T = m_T^2 = A_\lambda^2 = (200 \text{ GeV})^2$, for various values of M_T. As expected, for larger values of M_T, there is a thicker band on the $\mu - \tan\beta$ plane that is allowed.

We will quantify the degree of fine-tuning in the cancellation for allowed $\alpha\Delta T$ in Sec. IV. For now, we may estimate the fine-tuning along the ideas of Athron *et al.* [50]. For example, with the parameters that require a fine-tuning in M_T

$$\tan\beta = 3, \qquad \lambda = 0.9, \qquad \mu = 150 \text{ GeV}, \qquad m_T^2 = B_T = A_\lambda^2 = (200 \text{ GeV})^2, \tag{37}$$

we have viable ΔT in the regions

$$250 \text{ GeV} < M_T < 375 \text{ GeV}, \quad \text{or} \quad M_T > 3.0 \text{ TeV}. \tag{38}$$

For M_T below 3.0 TeV, we would typically have unacceptably large ΔT that violates precision electroweak constraints except in the a small region of M_T between 250 GeV and 375 GeV because of cancellations in the numerator of Eq. (36). If we sample M_T at random in the range between 0 and 3.0 TeV, the only region with viable ΔT is only 125(= 375 − 250) GeV wide, and we can thus estimate the fine-tuning as

$$\frac{3.0 \text{ TeV}}{375 \text{ GeV} - 250 \text{ GeV}} = 24, \tag{39}$$

so a cancellation of 1 part in 24 is required to have small $\alpha\Delta T$ for the parameters in Eq. (37).

E. Neutralino and charginos

After EWSB, the neutralino ($\tilde{N}$) and chargino ($\tilde{C}$) mass matrices are now extended with the triplet sector. The mass matrix for the neutralinos in the basis ($\tilde{b}$, $\tilde{w}^0$, $\tilde{H}_d^0$, $\tilde{H}_u^0$, $\tilde{T}^0$) is given by

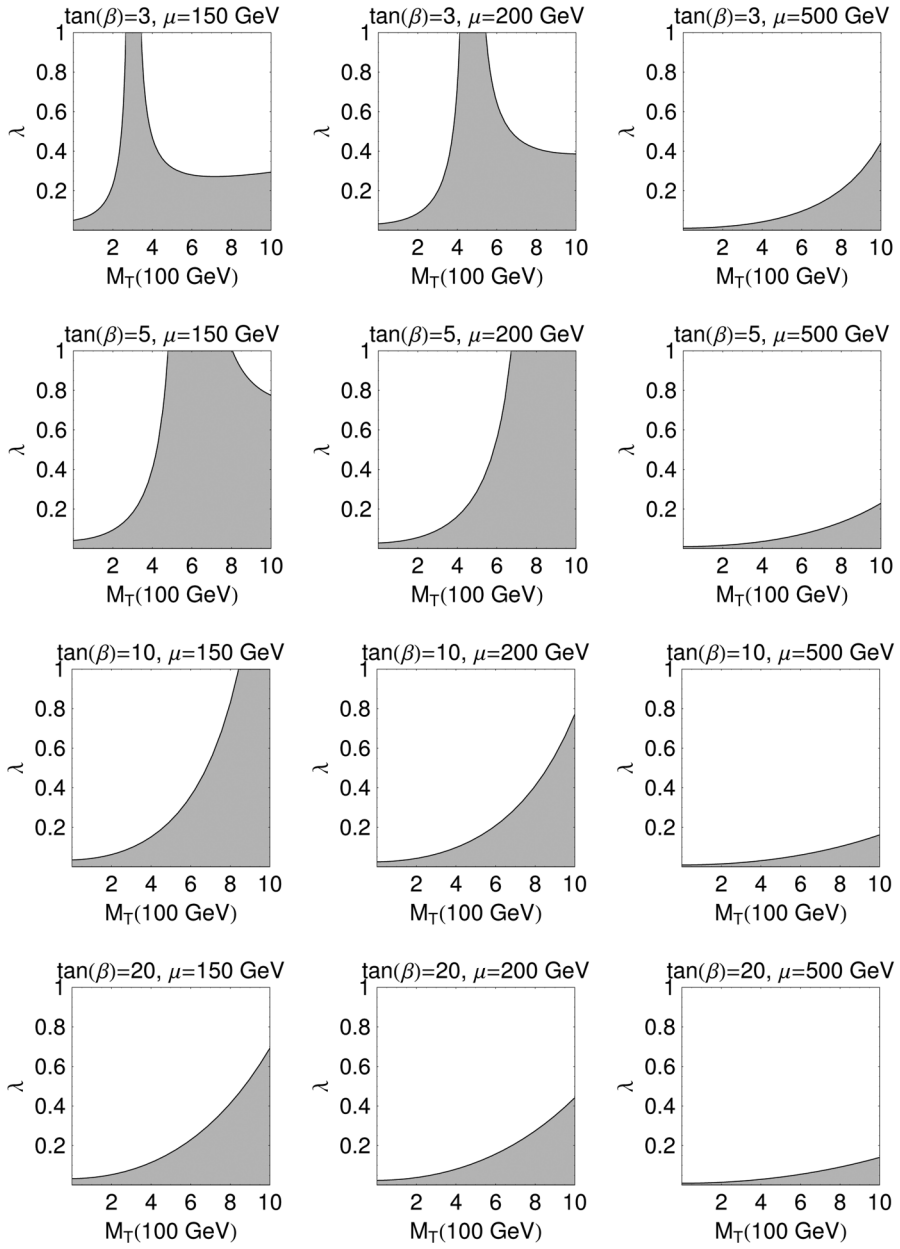

FIG. 2. Regions allowed by ΔT (in gray) on $\lambda - M_T$ plane for various values of $\tan\beta$ and μ as indicated in each plot.

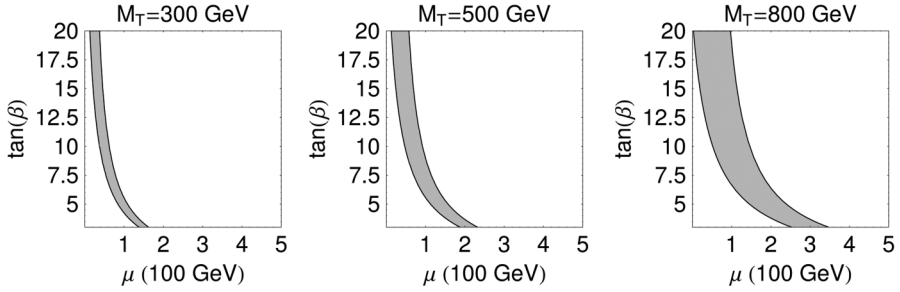

FIG. 3. Regions allowed by ΔT (in gray) on $\tan\beta - \mu$ plane for various values of M_T as indicated in each plot.

$$\mathcal{M}_{\tilde{N}} = \begin{pmatrix} M_1 & 0 & -\frac{1}{2}g_1 v_d & \frac{1}{2}g_1 v_u & 0 \\ 0 & M_2 & \frac{1}{2}g_2 v_d & -\frac{1}{2}g_2 v_u & 0 \\ -\frac{1}{2}g_1 v_d & \frac{1}{2}g_2 v_d & 0 & -\mu_{\rm eff} & \frac{1}{\sqrt{2}}\lambda v_u \\ \frac{1}{2}g_1 v_u & -\frac{1}{2}g_2 v_u & -\mu_{\rm eff} & 0 & \frac{1}{\sqrt{2}}\lambda v_d \\ 0 & 0 & \frac{1}{\sqrt{2}}\lambda v_u & \frac{1}{\sqrt{2}}\lambda v_d & M_T \end{pmatrix}, \tag{40}$$

where M_1 and M_2 are, respectively, the SUSY-breaking bino and wino masses, and $\mu_{\rm eff}$ is as defined in Eq. (30).

For the charginos, in the basis $\psi^{\pm} = (\tilde{w}^+, \tilde{H}_u^+, \tilde{T}^+, \tilde{w}^-, \tilde{H}_d^-, \tilde{T}^-)$, the chargino mass matrix appears in the Lagrangian as

$$\mathcal{L} \supset -\frac{1}{2}(\psi^{\pm})^T \begin{pmatrix} 0 & \mathcal{M}_{\tilde{C}}^T \\ \mathcal{M}_{\tilde{C}} & 0 \end{pmatrix} \psi^{\pm}, \tag{41}$$

where

$$\mathcal{M}_{\tilde{C}} = \begin{pmatrix} M_2 & \frac{\sqrt{2}}{2}g_2 v_d & g_2 v_t \\ \frac{\sqrt{2}}{2}g_2 v_u & \mu_{\rm eff} + \sqrt{2}\lambda v_t & -\lambda v_d \\ -g_2 v_t & \lambda v_u & M_T \end{pmatrix}. \tag{42}$$

III. LIGHTEST *CP*-EVEN HIGGS BOSON IN THE TESSM

A. Tree-level mass

The lightest *CP*-even Higgs boson in TESSM is a linear combination of the *CP*-even components of the Higgs doublets $H_{u,d}$ and the neutral component of the triplet T^0. After EWSB, the squared-mass matrix for the neutral scalar has the entries

$$\begin{aligned} (\mathcal{M}_a^2)_{11} &= c_\beta^2 M_A^2 + s_\beta^2 M_Z^2 - \frac{\lambda}{\sqrt{2}} t_\beta^{-1} v_t (M_T + A_\lambda), & (\mathcal{M}_a^2)_{12} &= -s_\beta c_\beta (M_A^2 + M_Z^2) + c_\beta s_\beta \lambda^2 v^2 + \frac{\lambda}{\sqrt{2}} v_t (M_T + A_\lambda), \\ (\mathcal{M}_a^2)_{13} &= \lambda v \left(\frac{1}{\sqrt{2}} (A_\lambda + M_T) c_\beta + (\lambda v_t - \sqrt{2}\mu) s_\beta \right) & (\mathcal{M}_a^2)_{22} &= s_\beta^2 M_A^2 + c_\beta^2 M_Z^2 - \frac{\lambda}{\sqrt{2}} t_\beta v_t (M_T + A_\lambda), \\ (\mathcal{M}_a^2)_{23} &= \lambda v \left(\frac{1}{\sqrt{2}} (A_\lambda + M_T) s_\beta + (\lambda v_t - \sqrt{2}\mu) c_\beta \right) & (\mathcal{M}_a^2)_{33} &= M_T^2 + m_T^2 + B_T + \frac{1}{2}\lambda^2 v^2, \end{aligned} \tag{43}$$

where v_t should be considered as a function of the input parameters via the minimization condition in Eq. (27) and we define M_A as in the case of the MSSM

$$M_A^2 \equiv 2\frac{B_\mu}{\sin 2\beta}. \tag{44}$$

As in the case of the NMSSM, the lightest mass-squared eigenvalue is bounded by the lightest eigenvalue of top-left 2×2 block of the mass matrix,

$$m_h^2 \leq M_Z^2 \left(\cos 2\beta + \frac{2\lambda^2}{g_2^2 + g_1^2} \sin 2\beta \right). \tag{45}$$

In Fig. 4, we plot this tree-level upper bound as a function of $\tan\beta$ for $\lambda = 0.7, 0.8$, and 0.9. For $\lambda = 0.9$, it is possible to obtain a tree-level Higgs mass larger than 100 GeV for $\tan\beta \lesssim 6$, and even satisfy the LEP2 bounds at tree-level for small $\tan\beta \lesssim 3.5$.

We can also see the MSSM limit in the mass matrix when the triplet decouples with fixed λ. In the limit $M_T \to \infty$, keeping all other parameters fixed, we have

$$M_T v_t \to -\frac{\lambda v^2}{2\sqrt{2}} \sin 2\beta, \tag{46}$$

and the mass matrix has the form

$$\mathcal{M}_a^2 \overset{M_T \to \infty}{\to} \begin{pmatrix} \mathcal{M}_{\rm MSSM}^2 + \Delta\mathcal{M}^2 & \epsilon \\ \epsilon^T & M_T^2 \end{pmatrix}, \tag{47}$$

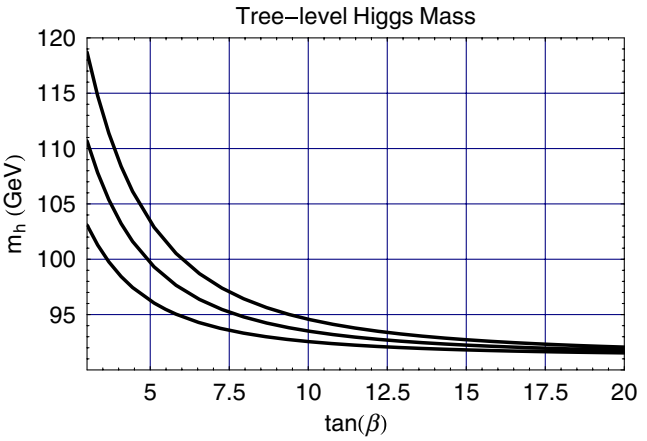

FIG. 4 (color online). Tree-level upper bound on the mass of the lightest *CP*-even Higgs boson as given by Eq. (45) as a function of $\tan\beta$ for $\lambda = 0.7$ (lowest line), 0.8 (middle line), and 0.9 (top line).

where $\mathcal{M}^2_{\rm MSSM}$ is the 2×2 MSSM mass matrix for the CP-even Higgs bosons, and

$$\Delta\mathcal{M}^2 = \lambda^2\frac{v^2}{2}\begin{pmatrix} c_\beta^2 & c_\beta s_\beta \\ c_\beta s_\beta & s_\beta^2 \end{pmatrix}, \tag{48}$$

$$\epsilon = \frac{\lambda}{\sqrt{2}} M_T v \begin{pmatrix} c_\beta \\ s_\beta \end{pmatrix}. \tag{49}$$

Integrating out the third row and column of the mass matrix in Eq. (47), the effective top-left 2×2 submatrix becomes

$$\begin{aligned}\mathcal{M}^2_{\rm eff} &= \mathcal{M}^2_{\rm MSSM} + \Delta\mathcal{M}^2 - \epsilon(M_T^2)^{-1}\epsilon^T + \mathcal{O}\left(\frac{\epsilon^3}{M_T^4}\right) \\ &= \mathcal{M}^2_{\rm MSSM} + \mathcal{O}\left(\frac{\lambda^3 v^3}{M_T}\right),\end{aligned} \tag{50}$$

and we recover the MSSM limit as $M_T \to \infty$. In Fig. 5, we show this decoupling behavior by plotting the tree-level mass of the lightest Higgs boson as a function of M_T for various values of $\tan\beta$, and see that, for $M_T \gtrsim 10^4$ GeV, we recover the MSSM results.

1. Numerical results

In this subsection, we numerically evaluate the mass of the lightest CP-even Higgs boson at tree level. With the minimization conditions, we can take as input parameters

$$\tan\beta,\ \mu,\ M_A,\ \lambda,\ M_T,\ m_T^2,\ B_T, \tag{51}$$

and fix $m^2_{H_u}$, $m^2_{H_d}$, and v_t by solving the minimization conditions with the experimental inputs of $M_Z = 91.19$ GeV and the gauge couplings $g_2(M_Z) \simeq 0.65$, $g_1(M_Z) \simeq 0.36$ (this fixes $v \simeq 245$ GeV). We discard sets of input parameters that give large v_t inconsistent with electroweak constraints. For all our numerical studies, we analyze two the cases of $\lambda = 0.8$ and $\lambda = 0.9$, and scan the parameter space in the range

$$\begin{aligned} &3 \le \tan\beta \le 30, \qquad 100\ \text{GeV} \le \mu, \\ &M_A \le 500\ \text{GeV}, \qquad 300\ \text{GeV} \le M_T \le 1000\ \text{GeV}, \\ &-2000\ \text{GeV} \le A_\lambda \le 2000\ \text{GeV}, \\ &-(1000\ \text{GeV})^2 \le m_T^2, \qquad B_T \le (1000\ \text{GeV})^2. \end{aligned} \tag{52}$$

The range of $\tan\beta$ is chosen so that the bottom Yukawa coupling is smaller than the top Yukawa coupling, and we can neglect the bottom Yukawa coupling when we study the production and decay properties of the lightest CP-even Higgs boson.

Since solutions to the minimization conditions only guarantee an extremum, we only keep solutions that give a local minimum by checking that all scalar masses are positive at the desired vev. We also discard any points that give unacceptably large $\alpha\Delta T$ or contain charged scalar particles lighter than 100 GeV.

For the range of parameters listed in Eq. (52), we show the mass of the lightest CP-even boson as a function of $\tan\beta$ in Fig. 6. In Fig. 6, we also plot the upper bound of the tree-level Higgs mass given in Eq. (45). The plots show that we can indeed achieve large (greater than M_Z) tree-level Higgs mass with large λ, and we can even satisfy LEP2 bounds at tree level for small values of $\tan\beta$ ($\tan\beta \lesssim 3.5$) when $\lambda = 0.9$.

B. Mass at the one-loop level

Since the lightest CP-even Higgs boson is a linear combination of a_i' for $i = u,\ d,\ t$ we will construct the Coleman-Weinberg (CW) potential [51] only for the fields

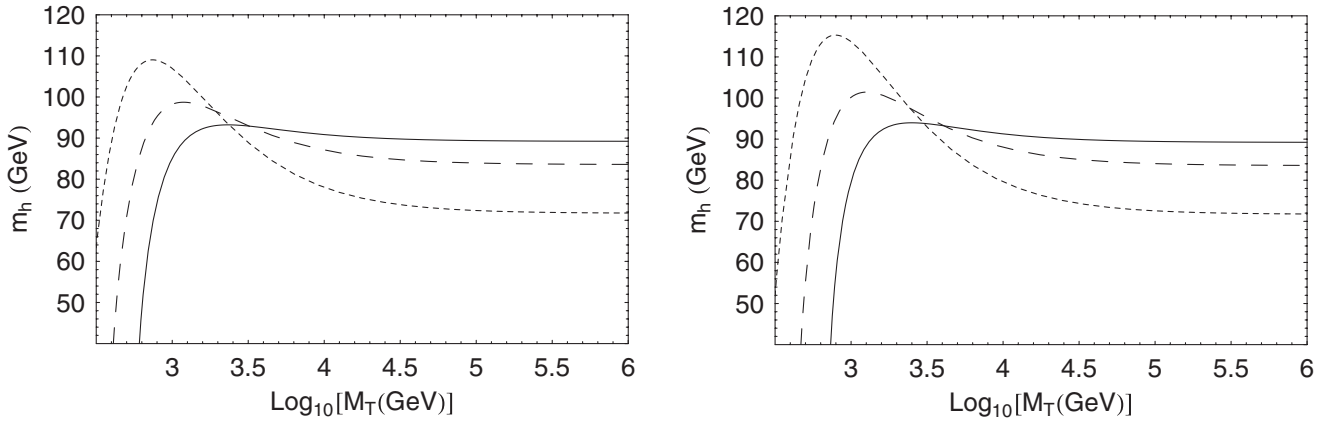

FIG. 5. Tree-level mass of the lightest CP-even Higgs boson as a function M_T for $\lambda = 0.8$ (left panel) and $\lambda = 0.9$ (right panel). The other parameters are kept fixed as $A_\lambda = m_T^2 = B_T = 0$, $\mu = 200$ GeV, and $M_A = 300$ GeV. The three curves have values of $\tan\beta$ of 10 (solid line), 5 (dashed line), and 3 (dotted line). For each case, we see decoupling in large M_T, and the limiting value agrees with the MSSM result.

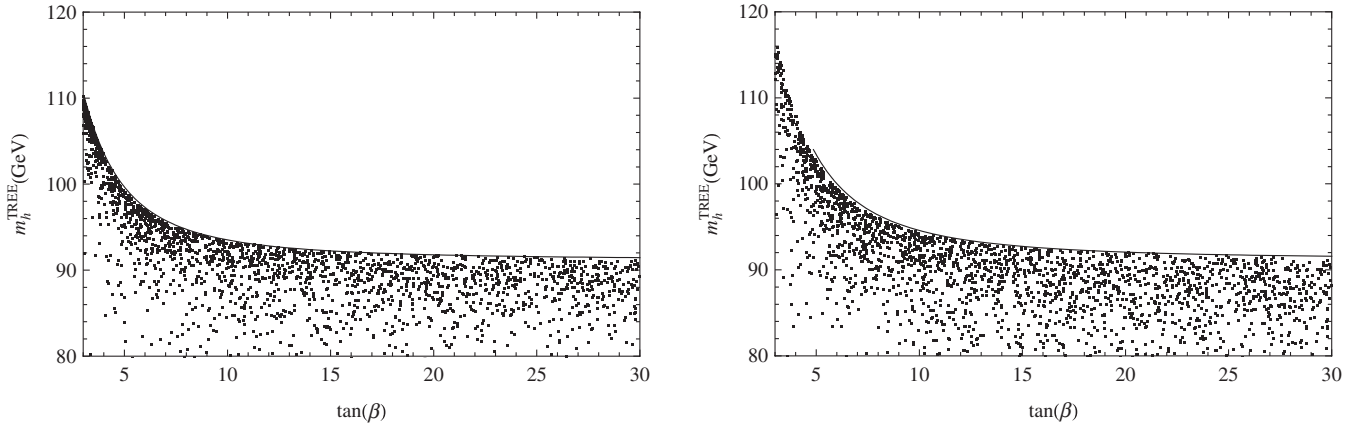

FIG. 6. Tree-level mass of the lightest CP-even Higgs boson as a function tanβ scanned over the parameter space as listed in Eq. (52). The plot on the left (right) has $\lambda = 0.8$ ($\lambda = 0.9$), and the top curve indicates the upper bound as computed from Eq. (45).

a_i, and extract the corrections to m_h^2 from the CW potential. Furthermore, we will make the two following assumptions:

(i) We assume that both the s-top masses are close to the top-quark mass, and the famous $\mathcal{O}(y_t^4)$ contributions in the MSSM are small. In other words, we only consider the corrections from the Higgs boson, neutralino, and chargino sectors. These contributions are dominated by the coupling λ and the SUSY-breaking parameters in the triplet sector. Our results will show that these contributions are sufficient to satisfy the LEP2 bounds on the Higgs mass, and we do not need large contributions from the top–s-top sector as in the case of the MSSM.

(ii) In the neutralino and chargino mass matrices, we ignore the mixing induced by gauge interactions. This removes dependencies on the bino and wino SUSY-breaking masses in our analysis as we do not include the bino and wino states, and we expect their contributions to be small when $M_{1,2} \sim M_Z$. (If we include the bino and wino states, we would also have to include the corresponding superpartners in the W and Z gauge bosons.)

The Coleman-Weinberg potential is given by

$$V_{\mathrm{CW}} = \frac{1}{64\pi^2}\,\mathrm{S\,Tr}\left[\mathcal{M}^4\left(\ln\frac{\mathcal{M}^2}{\mu_r^2} - \frac{3}{2}\right)\right], \tag{53}$$

where $\mathcal{M}^2$ are field-dependent mass matrices in which the fields are not replaced with their vevs, μ_r is the renormalization scale, and the supertrace includes a factor of $(-1)^{2J}(2J+1)$ so that fermions contribute oppositely to bosons, and the spin degrees of freedoms are appropriately summed over. Since here we are only interested in the CW potential of the fields a_i that always appear in the combination $(a_i' + v_i)$, the field-dependent matrices for the charginos and neutralinos are simply those in Eqs. (40) and (42) with the vevs v_i replaced by the corresponding fields a_i.

For the scalars, the naive replace-vev-by-field method fails and we need to distinguish between the contributions from the minimization conditions and those from the replacement of the fields with their corresponding vevs. For example, while the (11)-element of the mass matrix of the CP-even neutral Higgs boson is

$$(\mathcal{M}_a^2)_{11} = c_\beta^2 M_A^2 + s_\beta^2 M_Z^2 - \frac{\lambda}{\sqrt{2}} t_\beta^{-1} v_t (M_T + A_\lambda), \tag{54}$$

$$= B_\mu \frac{v_d}{v_u} + \frac{1}{4}(g_2^2 + g_1^2) v_u^2 - \frac{\lambda}{\sqrt{2}} v_t (M_T + A_\lambda) \frac{v_d}{v_u}, \tag{55}$$

it is incorrect to have the field dependence

$$(\mathcal{M}_a^2)_{11} \neq B_\mu \frac{a_d}{a_u} + \frac{1}{4}(g_2^2 + g_1^2) a_u^2 - \frac{\lambda}{\sqrt{2}} a_t (M_T + A_\lambda) \frac{a_d}{a_u}, \tag{56}$$

because some of the vev dependence in Eq. (55) comes from the minimization conditions Eq. (28). The correct field-dependent (11)-element of the CP-even neutral Higgs boson is

$$(\mathcal{M}_a^2)_{11} = m_{H_u}^2 + \mu^2 + \frac{g_2^2 + g_1^2}{8}(3a_u^2 - a_d^2) + \frac{\lambda^2}{2}(a_d^2 + a_t^2) - \sqrt{2}\lambda\mu a_t, \tag{57}$$

where $m_{H_u}^2$ is related to the vevs (but not the fields) through the minimization condition in Eq. (28). In Appendix A, we give the field-dependent mass matrices used in the calculation of the Coleman-Weinberg potential.

Since the analytical results for the mass eigenvalues of the field-dependent matrices are complicated, we will compute the Higgs mass numerically. The one-loop mass matrix can be extracted from the Coleman-Weinberg potential by numerically evaluating the derivatives of the mass eigenvalues with respect to the fields about the vevs [24] (dropping the prefactor from the supertrace for convenience)

$$(\Delta \mathcal{M}_a^2)_{ij} = \frac{\partial^2 V_{\rm CW}(a)}{\partial a_i \partial a_j}\bigg|_{\rm vev} - \frac{\delta_{ij}}{\langle a_i \rangle}\frac{\partial V_{\rm CW}(a)}{\partial a_i}\bigg|_{\rm vev} \tag{58}$$

$$= \sum_k \frac{1}{32\pi^2}\frac{\partial m_k^2}{\partial a_i}\frac{\partial m_k^2}{\partial a_j}\ln\frac{m_k^2}{\mu_r^2}\bigg|_{\rm vev} + \sum_k \frac{1}{32\pi^2} m_k^2 \frac{\partial^2 m_k^2}{\partial a_i \partial a_j}\left(\ln\frac{m_k^2}{\mu_r^2} - 1\right)\bigg|_{\rm vev} - \sum_k \frac{1}{32\pi^2} m_k^2 \frac{\delta_{ij}}{\langle a_i \rangle}\frac{\partial m_k^2}{\partial a_i}\left(\ln\frac{m_k^2}{\mu_r^2} - 1\right)\bigg|_{\rm vev} \tag{59}$$

where the second term in Eq. (58) takes into account the shift in the minimization conditions, and $\{m_k^2\}$ is the set of mass eigenvalues that enter the Coleman-Weinberg potential. Our set of $\{m_k^2\}$ includes the eigenvalues of the mass matrices of the *CP*-even, *CP*-odd, and charged Higgs bosons, as well as the neutralinos and charginos mass matrices. These field-dependent mass matrices are given in Appendix A.

1. Numerical results

We numerically compute the mass of the lightest *CP*-even Higgs boson to one loop using the Coleman-Weinberg potential for the parameter space in Eq. (52). For the same input parameters that give rise to the tree-level results shown in Fig. 6, we show the corresponding Higgs mass computed to one loop in Fig. 7, and the difference between the loop-level and tree-level masses in Fig. 8. We use the value of M_T as the renormalization scale μ_r that enters the Coleman-Weinberg potential. From these plots, we see that the triplet sector can give a large contribution to the mass of the lightest *CP*-even Higgs boson, and we can satisfy the LEP bounds without the s-top contributions for all values of $\tan\beta$ in our scanned range.

In Table I, we give some sample points in our scan. Points 1 and 2 are sample points that have small fine-tuning [as will be defined later in Eq. (77)]. The TESSM can achieve small fine-tuning because the Higgs mass can be large at tree level and does not require large contributions from radiative corrections. Points 3 and 4 are samples of the points with the largest Higgs masses (and therefore fine-tuning) in our scanned range of parameter space, as evident in the values of SUSY-breaking parameters m_T^2, A_λ, and B_T being near the boundary of the scanned range. Points 5 and 6 are samples of points having a large $\tan\beta(\geq 20)$, where the tree-level Higgs mass is only slightly larger than M_Z, and there is a significant one-loop contribution, and, correspondingly, large fine-tuning.

C. Collider signatures of the lightest *CP*-even Higgs boson in TESSM

With large λ in both the TESSM and the NMSSM, we do not require heavy s-tops. In these cases, the gluon-gluon fusion production of the lightest *CP*-even Higgs boson, $\sigma(gg \to h)$, and its diphoton partial decay width, $\Gamma(h \to \gamma\gamma)$, can be very different from the MSSM because these processes involve s-top loops. In this section, we perform a simplified analysis showing that in the TESSM there may be a gluophilic Higgs boson whose gluon-gluon fusion production cross section can be larger than that of the SM by a factor of 1.8. As stated in the introduction, our discussions of the gluon-gluon fusion production rely only on the existence of light s-tops and the minimal color sector of the MSSM, and are therefore applicable to any extensions of the MSSM that solves the little hierarchy problem without invoking additional colored states. For the diphoton partial decay width, there are several sources of suppression, and we may have a partial decay width that is about 0.8 times that in the SM.

Of course, at the LHC the relevant quantity is the product of the gluon-gluon fusion production cross section and the diphoton branching ratio

$$\sigma(gg \to h)\mathrm{Br}(h \to \gamma\gamma),$$

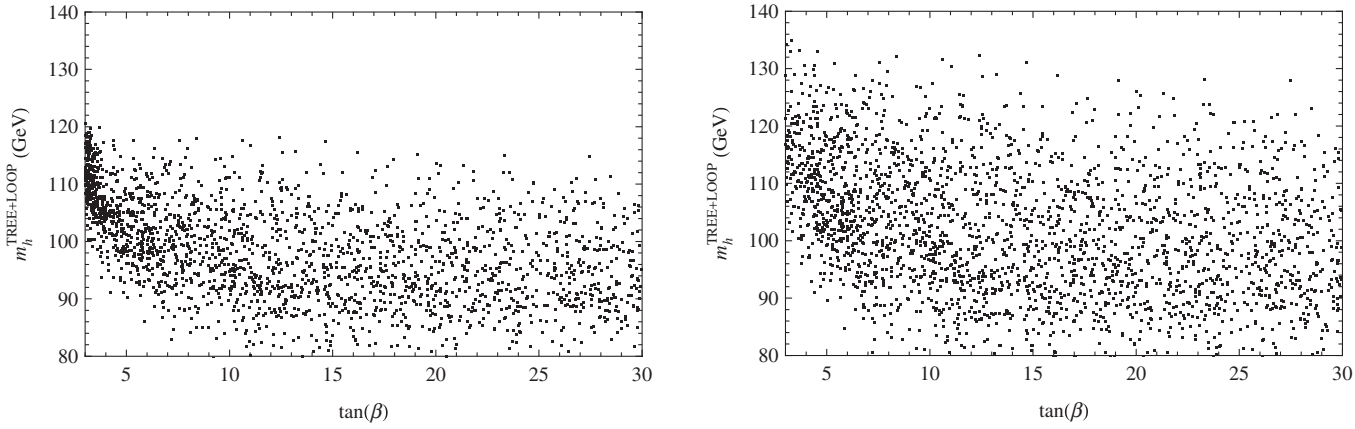

FIG. 7. Mass of the lightest *CP*-even Higgs boson, including one-loop contributions from the triplet sector, as a function $\tan\beta$, scanned over the parameter space as listed in Eq. (52). The plot on the left has $\lambda = 0.8$, and the plot on the right has $\lambda = 0.9$. The input parameters of the individual points are the same as those that give rise to the points shown in the corresponding plot of Fig. 6.

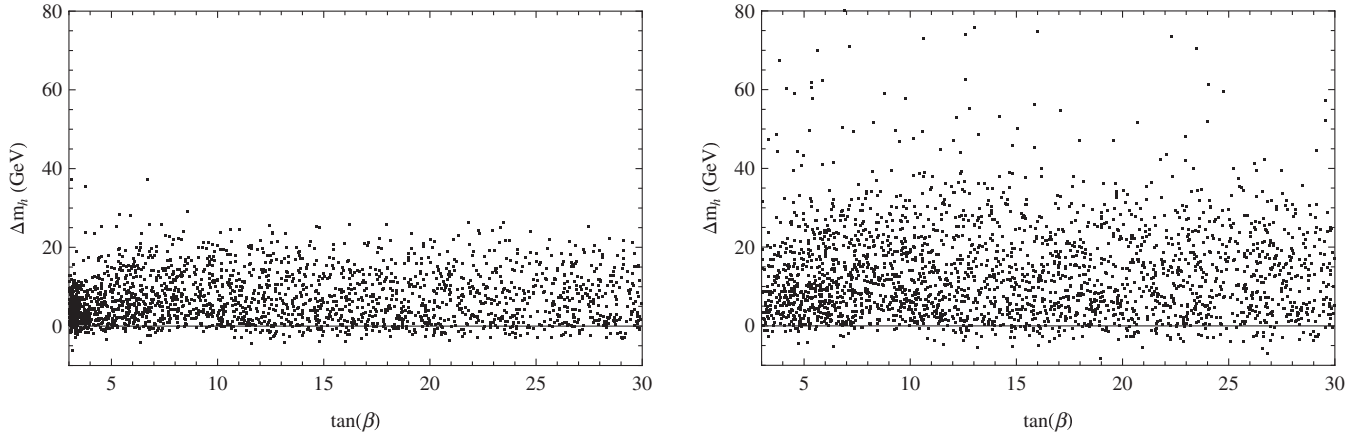

FIG. 8. Difference between the mass of the lightest CP-even Higgs boson with and without the one-loop contribution from the triplet sector for the points shown in the corresponding plots of Figs. 6 and 7. The plot on the left has $\lambda = 0.8$, and the plot on the right has $\lambda = 0.9$.

and a more complete analysis would have to take into account the effects of light s-tops to all the decay channels as well as the large, higher-loop corrections from QCD and large couplings. We leave the complete analysis of the Higgs production and decay for future work.

The well-known formula for the decay width of a real scalar decaying into two photons can be found in Gunion *et al.* [52]. This formula is also presented in the Appendix B.

1. Gluophilic Higgs boson

In the SM, ignoring all the Yukawa couplings except for the top Yukawa coupling, the process $h \rightarrow gg$ proceeds only through a top-quark loop. In the MSSM, we have additional contributions from the s-tops (see Fig. 9), as well as all the other s-quarks through D-term interactions of the form $h\tilde{q}^*\tilde{q}$ with coupling of the order M_Z. To simplify our analysis, we will ignore the D-term interactions except those in the s-top sector, but we note that these contributions can be important when there are light s-quarks and must be taken into account in a full analysis.

In the MSSM with small s-top mixing, the s-top contributions interfere constructively with the top-quark contribution for the gluon-gluon fusion production cross section [53,54]. However, with small s-top mixing, the s-tops need to be heavy to satisfy the LEP bounds on the Higgs mass,

TABLE I. Sample Higgs spectra. All dimensionful parameters are in units of GeV, except for m_T^2 and B_T, which are in units of $(\text{GeV})^2$. The definitions of fine-tuning f_T, κ_T, and κ_T' are given, respectively, in Eqs. (77), (79), and (80). The value of f_T indicates the percent change in v^2 induced by a 1% change in $m_{H_u}^2$ at a fundamental scale of SUSY breaking, and the value of κ_T indicates the percent change in ΔT induced by a 1% change in M_T. The measure κ_T' is only applicable to Points 1 and 2, and shows that there is a cancellation of one part in 23 to give a viable value of ΔT. Points 1 and 2 show examples of input parameters that give a viable Higgs mass with a small fine-tuning in the electroweak sector. Points 3 and 4 differ only in λ and are samples that give large Higgs masses of about 120 GeV (for $\lambda = 0.8$) and about 135 GeV (for $\lambda = 0.9$). Points 5 and 6 have large $\tan\beta(\geq 20)$ and $m_h \sim M_Z$ at tree level, but there are large radiative corrections to have viable Higgs masses at one loop.

	Point 1	Point 2	Point 3	Point 4	Point 5	Point 6
$\tan\beta$	3.20	3.20	3.20	3.20	20.0	27.7
μ	270	270	400	400	200	165
M_A	430	430	280	280	300	410
λ	0.8	0.9	0.8	0.9	0.8	0.9
M_T	370	400	400	400	350	330
m_T^2	$(500)^2$	$(280)^2$	$(1970)^2$	$(1970)^2$	$(1600)^2$	$(1500)^2$
A_λ	600	460	1860	1860	1800	1300
B_T	$(400)^2$	$(400)^2$	$(1730)^2$	$(1730)^2$	$(500)^2$	$(1400)^2$
m_h^{Tree}	108	113	105	111	88	90
$m_h^{\text{Tree+Loop}}$	114	117	122	137	114	121
f_T	33	19	399	505	315	271
κ_T	33	11	0.8	0.8	0.5	0.3
κ_T'	4.7	6.4				

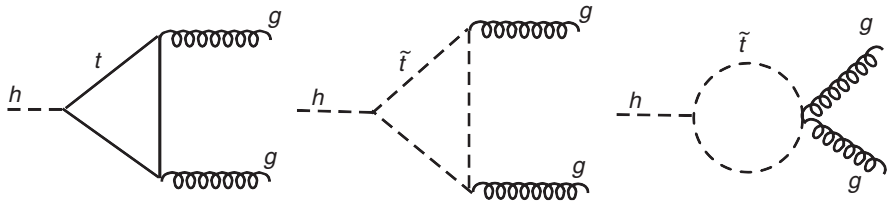

FIG. 9. The diagrams that contribute to the amplitude $\mathcal{A}(h \to gg)$ in the TESSM.

and the s-top contributions decouple. (With large-stop mixing, it is possible to have s-top contributions that interfere destructively with the top-quark contribution, leading to a gluophobic Higgs boson.)

In the TESSM and NMSSM, we can have light s-tops at the expense of perturbativity at the GUT scale, and a large enhancement in the production rate. Assuming large $\tan\beta$ so that $v \simeq v_u$ and there is no s-top mixing, and approximating the lightest CP-even Higgs boson h as being dominantly composed of a'_u (the CP-even component of H_u), we have the interactions

$$-\mathcal{L} \supset \frac{y_t}{\sqrt{2}} h\bar{t}t + \left(y_t^2 + \frac{1}{12}g_1^2 - \frac{1}{4}g_2^2\right) v h \tilde{Q}_3^* \tilde{Q}_3 + \left(y_t^2 - \frac{1}{3}g_1^2\right) v h \tilde{\bar{U}}_3^* \tilde{\bar{U}}_3, \tag{60}$$

where t is the top quark, and $\tilde{Q}_3$ ($\tilde{\bar{U}}_3$) is the superpartner to the left-(right-)handed component of the top quark. From Eqs. (B2), (B9), and (B10), the ratio of the amplitudes $\mathcal{A}(gg \to h)$ due to the s-top s-quarks and top quark is then

$$r_{gg\to h} \equiv \frac{\mathcal{A}_{\tilde{t}}}{\mathcal{A}_t} = \frac{m_t^2 + \frac{1}{4}(\frac{1}{6}g_1^2 - \frac{1}{2}g_2^2)v^2}{m_{\tilde{Q}_3}^2 + m_t^2}\frac{F_{\tilde{Q}_3}}{F_t} + \frac{m_t^2 - \frac{1}{6}g_1^2 v^2}{m_{\tilde{\bar{U}}_3}^2 + m_t^2}\frac{F_{\tilde{\bar{U}}_3}}{F_t}, \tag{61}$$

where $m_{\tilde{Q}_3}^2$ and $m_{\tilde{\bar{U}}_3}^2$ are SUSY-breaking soft masses of the corresponding s-tops, and we have used the relationships $m_t = (\sqrt{2})^{-1} y_t v_u$. In Fig. 10, we plot $r_{gg\to h}$ as a function of a common soft s-top mass $m_{\tilde{Q}_3}^2 = m_{\tilde{\bar{U}}_3}^2 = m_{\mathrm{SUSY}}^2$, assuming $m_h = 114$ GeV. Since the s-top mass eigenvalues in this simplified analysis are given by

$$m_{\tilde{t}}^2 = m_{\mathrm{SUSY}}^2 + m_t^2, \tag{62}$$

and the current searches limit the s-tops masses to be greater than 120 GeV [55], we can have $m_{\mathrm{SUSY}} \sim 0$ (so $m_{\tilde{t}} = m_t$) and $r_{gg\to h}$ can be as large as 0.48. This gives a gluophilic Higgs boson whose production cross section via gluon-gluon fusion may be enhanced relative to the SM prediction by a factor of $(1.48)^2 \sim 2.2$.

Imposing perturbativity at the GUT scale, we can have a milder gluophilic Higgs boson when one of the s-top is light (the other is required to be heavy to have a Higgs mass satisfying the LEP2 bounds). However, when only one s-top is light, the enhancement in the gluon-gluon fusion production cross section is only a factor of $(1 + 0.5 \times 0.48)^2 \sim 1.5$ larger than that of the SM.

2. Diphoton decay of the Higgs boson

In the SM, the diphoton decay of the Higgs boson proceeds through W-boson loop in addition to top-quark loop, and the contribution from the top quark destructively interferes with the dominant W-boson contribution. In the MSSM, we have additional contributions from the s-tops and charginos (the corresponding superpartners of the top quark and W-boson), and, as in the case of $\Gamma(h \to gg)$, contributions from all the electrically charged s-quarks and s-leptons through D-term interactions.

In the TESSM, we have the additional contributions from the states composed dominantly of the charged triplets, and also new contributions from the MSSM matter content induced by λ (see Fig. 11). These contributions may be important when λ is as large as the top Yukawa coupling, and so in this subsection we use $\lambda = 0.9$ for our numerical studies. In this work, we will simplify our analysis by ignoring contributions from the D-term interactions except those involving the s-tops, and, using the same approximations as in the previous subsection of large $\tan\beta$ and $h \simeq a'_u$, we have the interactions and fermion masses

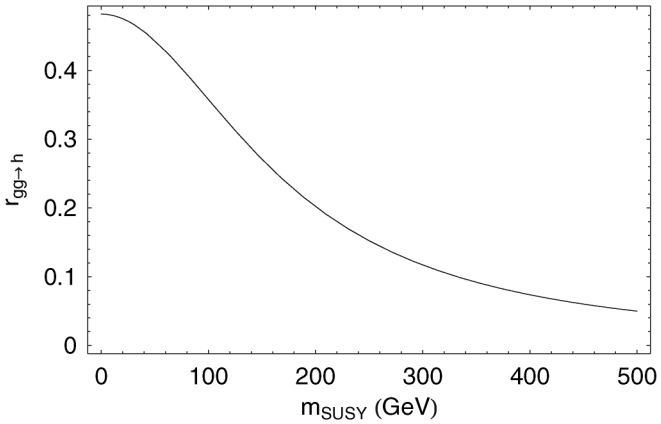

FIG. 10. The amplitude $\mathcal{A}(gg \to h)$ through s-top loops normalized with respect to the amplitude through top-quark loop, as a function of a common s-top soft mass $m_{\tilde{t}}$, assuming no mixing in the s-top sector.

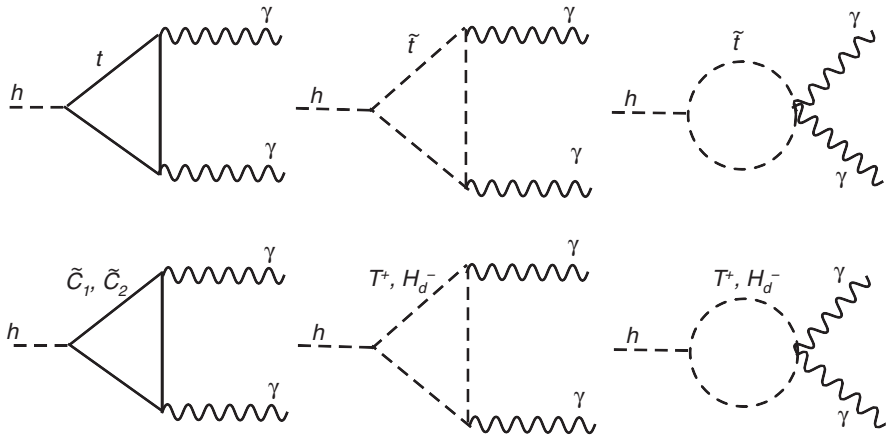

FIG. 11. The diagrams that contribute to the amplitude $\mathcal{A}(h \to \gamma\gamma)$ in the TESSM. The top three diagrams are present in the MSSM, and the bottom three diagrams involve the coupling λ.

$$
\begin{aligned}
-\mathcal{L} \supset\ & 2\lambda^2 v h(|T^+|^2 + |H_d^-|^2) \\
& + \lambda(h + v)(\bar{\tilde{H}} P_L \tilde{T}^+ + \bar{\tilde{T}} P_R \tilde{H}^+) \\
& + \mu(\bar{\tilde{H}}\tilde{H}^+) + M_T(\bar{\tilde{T}}\tilde{T}^+),
\end{aligned} \tag{63}
$$

where $\tilde{H}^+$ and $\tilde{T}^+$ are Dirac spinors formed from the Higgsinos and the fermionic components of the charged triplet states

$$
\tilde{H}^+ \equiv \begin{pmatrix} \tilde{H}_u^+ \\ \tilde{H}_d^{-\dagger} \end{pmatrix}, \qquad \tilde{T}^+ \equiv \begin{pmatrix} \tilde{T}^+ \\ \tilde{T}^{-\dagger} \end{pmatrix}, \tag{64}
$$

and $P_{L,R}$ are the projection operators

$$
P_L \equiv \begin{pmatrix} 1 & 0 \\ 0 & 0 \end{pmatrix}, \qquad P_R \equiv \begin{pmatrix} 0 & 0 \\ 0 & 1 \end{pmatrix}. \tag{65}
$$

Although none of the charged states in Eq. (63) is a mass eigenstate, we approximate the scalar states as mass eigenstates with masses

$$
m_{T^+}^2 \simeq M_T^2 + m_T^2, m_{H_d^-}^2 \simeq M_A^2, \tag{66}
$$

so that the contributions of these states to the amplitude $\mathcal{A}(h \to \gamma\gamma)$ have the same form. In the fermionic sector, the contribution to the amplitude $\mathcal{A}(h \to \gamma\gamma)$ comes exclusively from the mixing between $\tilde{H}^+$ and $\tilde{T}^+$. We can diagonalize the fermionic mass matrix with two unitary transformations

$$
\begin{aligned}
& \begin{pmatrix} \bar{\tilde{H}} \\ \bar{\tilde{T}}^+ \end{pmatrix}^T V^\dagger V \begin{pmatrix} \mu & \lambda v \\ 0 & M_T \end{pmatrix} U^\dagger U P_L \begin{pmatrix} \tilde{H}^+ \\ \tilde{T}^+ \end{pmatrix} \\
& = \begin{pmatrix} \bar{\tilde{C}}_1 \\ \bar{\tilde{C}}_2 \end{pmatrix}^T \begin{pmatrix} m_{\tilde{C}_1} & 0 \\ 0 & m_{\tilde{C}_2} \end{pmatrix} P_L \begin{pmatrix} \tilde{C}_1 \\ \tilde{C}_2 \end{pmatrix},
\end{aligned} \tag{67}
$$

where U and V are, respectively, parameterized by φ and φ',

$$
U \equiv \begin{pmatrix} c_\varphi & -s_\varphi \\ s_\varphi & c_\varphi \end{pmatrix}, \qquad V \equiv \begin{pmatrix} c_{\varphi'} & -s_{\varphi'} \\ s_{\varphi'} & c_{\varphi'} \end{pmatrix}, \tag{68}
$$

where $c_\varphi = \cos\varphi$ and $s_\varphi = \sin\varphi$, and $c_{\varphi'}$ and $s_{\varphi'}$ are similarly defined. These mixing angles are given by

$$
\begin{aligned}
\tan 2\varphi &= \frac{2\lambda\mu v}{M_T^2 - \mu^2 + \lambda^2 v^2}, \\
\tan 2\varphi' &= \frac{2\lambda v M_T}{M_T^2 - \mu^2 - \lambda^2 v^2}.
\end{aligned} \tag{69}
$$

In terms of the mass eigenstates and mixing angles, the chargino interactions in Eq. (63) take the form

$$
\begin{aligned}
-\mathcal{L} \supset\ & \lambda h(-c_{\varphi'} s_\varphi \bar{\tilde{C}}_1 \tilde{C}_1 + c_\varphi s_{\varphi'} \bar{\tilde{C}}_2 \tilde{C}_2) \\
& + \lambda h(c_{\varphi'} c_\varphi \bar{\tilde{C}}_1 P_L \tilde{C}_2 - s_\varphi s_{\varphi'} \bar{\tilde{C}}_2 P_L \tilde{C}_1 + \text{H.c.}).
\end{aligned} \tag{70}
$$

In Figs. 12 and 13, we illustrate the contributions of light s-tops and the additional charged states to the diphoton partial decay width, normalized with respect to the dominant W-boson contribution, assuming $m_h = 114$ GeV. In Fig. 12, we show the contributions from the top quark (constant line), s-tops (solid line), and the charged scalar states (dotted line). For the s-tops (charged scalar states H_d^- and T^+), the horizontal axis should be interpreted as a common soft SUSY-breaking mass M_{SUSY} (mass of these charged scalar states). In Fig. 13, we show the sum of the fermion contributions as a function of M_T for different values of μ, and see that even for small values of μ and M_T (μ, $M_T \lesssim 200$ GeV), these contributions tend to be small. We can partially attribute the smallness to a cancellation between the contributions from the two states $\tilde{C}_1$ and $\tilde{C}_2$, as evident in the relative sign difference between the coefficients of the $h\bar{\tilde{C}}_1\tilde{C}_1$ and $h\bar{\tilde{C}}_2\tilde{C}_2$ interactions. Though these fermionic contributions are small, it is interesting to note that, while the top-quark contribution interferes de-

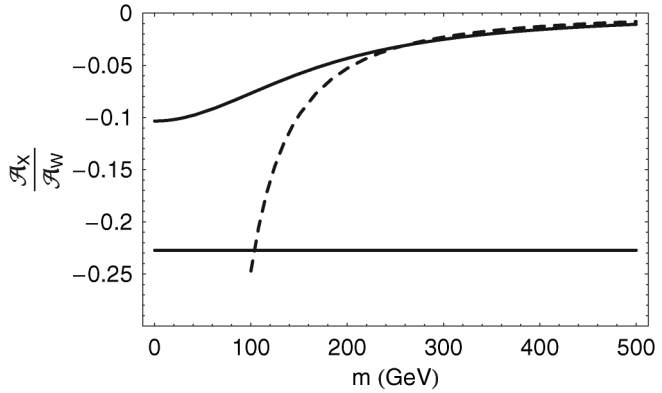

FIG. 12. The ratio of amplitudes $\mathcal{A}(h \to \gamma\gamma)$ through scalar s-tops, H_d^-, and T^+ loops, compared to the dominant W-boson loop contribution, as a function, respectively, of a common soft mass for the s-top (solid curve), and of the mass of the states H_d^- and T^+ (dashed line). We use $\lambda = 0.9$. The constant, solid line denotes the top-quark contribution.

structively with the W-boson contribution, the sum of these fermionic contributions interferes constructively. In any case, the additional λ-induced contributions (both bosonic and fermionic) to the partial decay width $\Gamma(h \to \gamma\gamma)$ are small compared to the s-top contributions.

Combining all these contributions to $\mathcal{A}(h \to \gamma\gamma)$, the diphoton partial width can be significantly reduced (mostly from the s-top contributions). For example, with $M_{\rm SUSY}^2 = m_T^2 = 0$, $\mu = 150$ GeV, $M_A = 200$ GeV, and $M_T = 500$ GeV, the amplitude $\mathcal{A}(h \to \gamma\gamma)$ is decreased by (relative to the SM) a factor of

$$\frac{\mathcal{A}_W + \mathcal{A}_t + \mathcal{A}_{\tilde{t}} + \mathcal{A}_{H_d^-} + \mathcal{A}_{T^+} + (\mathcal{A}_{\tilde{C}_1} + \mathcal{A}_{\tilde{C}_2})}{\mathcal{A}_W + \mathcal{A}_t} \sim \frac{1 - 0.23 - 0.11 - 0.05 - 0.008 + 0.001}{1 - 0.23} \sim 0.78,$$

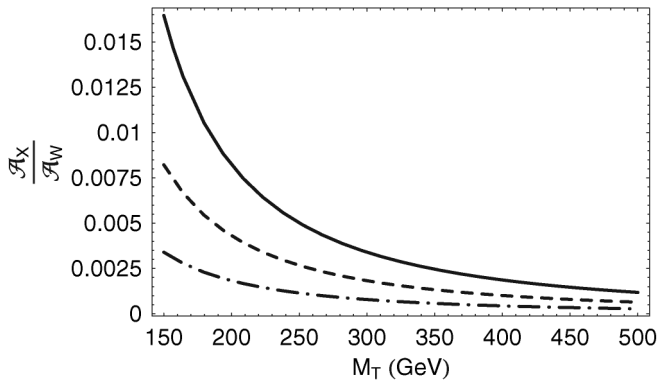

FIG. 13. The sum of amplitudes $\mathcal{A}(h \to \gamma\gamma)$ given by $\tilde{C}_1$ and $\tilde{C}_2$ loops normalized to the dominant W-boson loop amplitude, as a function of M_T for $\mu = 150$ GeV (solid line), 200 GeV (dashed line), and 300 GeV (dot-dashed line). Note that these fermionic contributions are small compared to the s-top contributions shown in Fig. 12.

and the diphoton decay partial width is decreased, relative to the SM partial decay width, by a factor of $(0.78)^2 \simeq 0.6$. We therefore can have a photophobic Higgs boson in the TESSM from the contribution of light s-tops.

IV. FINE-TUNINGS IN TESSM

A. Electroweak sector

Before discussing the fine-tuning in the electroweak sector of the TESSM, we briefly review the little hierarchy problem in the MSSM. In the MSSM with large $\tan\beta$, the Higgs doublet H_u is responsible for most of the EWSB since $v \simeq \sqrt{2}\langle H_u \rangle$, and it has the potential

$$V_{H_u} = (m_{H_u}^2 + \mu^2)|H_u|^2 + \tfrac{1}{8}(g_2^2 + g_1^2)|H_u|^4. \tag{71}$$

Minimizing the potential then gives

$$2\langle H_u^2 \rangle = v_u^2 = -8\frac{m_{H_u}^2 + \mu^2}{g_2^2 + g_1^2}, \tag{72}$$

so that

$$m_{H_u}^2 = -\tfrac{1}{8}(g_2^2 + g_1^2)v_u^2 - \mu^2. \tag{73}$$

Under radiative corrections, $m_{H_u}^2$ receives large logarithmic corrections from the s-top sector, and we can use the renormalization group equations to infer the value of $m_{H_u}^2$ at a fundamental scale Λ,

$$m_{H_u}^2(\Lambda) \simeq m_{H_u}^2(M_Z) + \frac{3y_t^2}{8\pi^2}\left(m_{\tilde{Q}_3}^2 + m_{\tilde{U}_3}^2 + A_t^2\right)\left(\ln\frac{\Lambda}{M_Z}\right), \tag{74}$$

where $m_{\tilde{Q}_3}^2$ and $m_{\tilde{U}_3}^2$ are the SUSY-breaking s-top masses, $y_t A_t$ is the coupling of the trilinear interaction $\tilde{Q}_3 H_u \tilde{U}_3$, and Λ can be taken as the scale of SUSY breaking. The large radiative correction leads to fine-tuning f_s because the electroweak scale v depends sensitively on the value of $m_{H_u}^2$ at the fundamental scale of SUSY breaking Λ. We can quantify this fine-tuning as [56]

$$f_s \equiv \frac{\delta \ln v^2}{\delta \ln m_{H_u}^2(\Lambda)} \simeq \frac{3y_t^2}{4\pi^2}\left(\frac{m_{\tilde{Q}_3}^2 + m_{\tilde{U}_3}^2 + A_t^2}{M_Z^2}\right)\left(\ln\frac{\Lambda}{M_Z}\right). \tag{75}$$

As a reference of comparison, for $m_{\tilde{Q}_3}^2 = m_{\tilde{U}_3}^2 = A_t = 1$ TeV, and $\Lambda = 10^3$ TeV, we have $f_s = 80$ so that the Higgs sector needs to be fine-tuned to one part in 80. Thus, even though the electroweak scale is no longer quadratically sensitive to the fundamental scale Λ with softly broken SUSY, it is quadratic sensitive to the s-top masses and trilinear coupling A_t, which are required to be large to have a Higgs mass that satisfies the LEP bounds, and this leads to a fine-tuning in the Higgs sector of about one part in 100. This is the little hierarchy problem in the MSSM.

We can also define other measures of fine-tuning when given a more fundamental theory (for example, an organizing principle of the soft SUSY-breaking parameters)

[50,57,58]. However, in this work we are mainly interested in the low-energy phenomenology of the TESSM without appealing to a particular fundamental theory, and we will simply define fine-tuning as in Eq. (75).

In the TESSM with λ comparable to the top Yukawa coupling, we do not need heavy s-top masses nor significant mixing in the s-top sector for the Higgs mass to satisfy the LEP bound, and as such there is little or no fine-tuning from the s-top sector. On the other hand, $m_{H_u}^2$ now receives radiative corrections from the triplet sector as well as the s-top sector

$$m_{H_u}^2(\Lambda) \simeq m_{H_u}^2(M_Z) + \frac{3y_t^2}{8\pi^2}(m_{\tilde{Q}_3}^2 + m_{\tilde{U}_3}^2 + A_t^2)\left(\ln\frac{\Lambda}{M_Z}\right) + \frac{3\lambda^2}{8\pi^2}(m_T^2 + A_\lambda^2)\left(\ln\frac{\Lambda}{M_Z}\right), \tag{76}$$

and we can follow the same steps and reasoning as before to have an estimate of the fine-tuning due to the triplet sector f_T

$$f_T \simeq \frac{3\lambda^2}{4\pi^2}\left(\frac{m_T^2 + A_\lambda^2}{M_Z^2}\right)\left(\ln\frac{\Lambda}{M_Z}\right), \tag{77}$$

so that $f_T = 40$, for example, would mean a tuning in $m_{H_u}^2(\Lambda)$ to one part in 40. The value of f_T indicates the percent change in v^2 per a one-percent change in $m_{H_u}^2$ at a fundamental scale of SUSY breaking, Generally, with large λ, for a given mass of the lightest CP-even Higgs boson, the fine-tuning in $m_{H_u}^2$ is less in the TESSM than the MSSM. In Fig. 14, we plot f_T for the data points shown in Fig. 7, where we see a rough general trend of increasing fine-tuning with increasing Higgs mass. On the other hand, it is possible to have points with relatively small $f_T (f_T \lesssim 20)$ that satisfy the LEP2 bound of $m_h > 114.4$ GeV, as demonstrated in Point 1 of Table I. This is a great improvement over the MSSM, and it is a consequence of the large tree-level mass we can obtain in TESSM, so we do not have to rely on large radiative corrections from m_T^2 and A_λ.

B. Triplet sector

The vev of T^0 is induced by the vevs of the Higgs doublets because the vevs of the Higgs doublets $v_{u,d}$ induce a tadpole from the trilinear interactions of the form HTH in the second line of Eq. (12). We noted earlier that some cancellation between *a priori* unrelated parameters (μ and $M_T \sin 2\beta$, for example) is required to keep v_t (and thus ΔT) small and this leads to fine-tuning in the triplet sector. However, it is worth pointing out that v_t here does not receive a large radiative correction that requires a fine-tuning as severe as the fine-tuning in the hierarchy problem in the triplet-extended standard model potential analyzed in Chivukula *et al.* [34]. It is easiest to see this in the limit $m_T^2 = B_T = A_\lambda^2 = 0$ (SUSY limit in the triplet sector) where the triplet vev v_t in Eq. (27) takes a particularly simple form

$$v_t = \frac{\sqrt{2}}{2}(\lambda v^2)\frac{\mu - M_T s_\beta c_\beta}{M_T^2 + \frac{\lambda^2}{2}v^2}, \tag{78}$$

and the 1-loop corrections to v_t then involve 1-loop corrections to the parameters λ, $v_{u,d}$, and M_T. The parameters λ, μ, and M_T come from the superpotential, and the non-renormalization theorem dictates that the radiative corrections to these parameters run only in a logarithmical manner due to wave function renormalizations only. Though the loop corrections to $v_{u,d}$ may require a fine-tuning of one part in a few hundreds (this is the little hierarchy problem in the MSSM), this is much more benign than the fine-tuning in the triplet-extended SM studied in Chivukula *et al.* [34].

On the other hand, there is a source of fine-tuning in v_t because we often require some degree of cancellation to make ΔT small. We can define a quantitative measure of fine-tuning in ΔT by

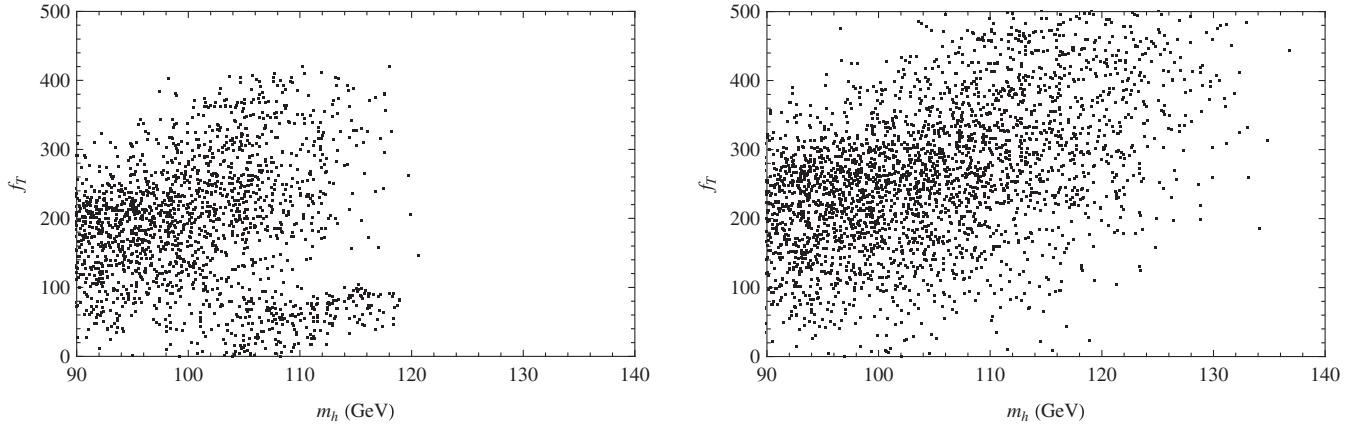

FIG. 14. Fine-tuning [as defined in Eq. (77)] as a function of the mass lightest CP-even Higgs boson. This is typically less than the fine-tuning of the MSSM [as defined in Eq. (75)] and the NMSSM. The plot on the left has $\lambda = 0.8$, and the plot on the right has $\lambda = 0.9$.

$$\kappa_T \equiv \frac{\delta \ln \Delta T}{\delta \ln M_T} = 2\frac{\delta \ln v_t}{\delta \ln M_T} = \left(\frac{2M_T}{\sin 2\beta(A_\lambda + M_T) - 2\mu}\right)\left(\frac{4\mu M_T + \sin 2\beta(m_T^2 + B_T - 2A_\lambda M_T - M_T^2 + \frac{\lambda^2}{2}v^2)}{M_T^2 + m_T^2 + B_T + \frac{\lambda^2}{2}v^2}\right), \quad (79)$$

so that κ_T is large when there is a large cancellation in the combination

$$\sin 2\beta(A_\lambda + M_T) - 2\mu,$$

that makes ΔT unnaturally small.

The definition in Eq. (79), however, may not be satisfactory because it does not take into account the range of allowed ΔT. For example, for the parameters listed in Eq. (37)

$$\tan\beta = 3, \quad \lambda = 0.9, \quad \mu = 150 \text{ GeV},$$
$$m_T^2 = B_T = A_\lambda^2 = (200 \text{ GeV})^2,$$

we have viable ΔT in the regions

$$250 \text{ GeV} < M_T < 375 \text{ GeV}, \quad \text{or} \quad M_T > 3.0 \text{ TeV},$$

and it may be reasonable to expect that any value of M_T in the small range between 250 GeV and 375 GeV is equally fine-tuned. However, Eq. (79) would give different values of κ_T for different values of M_T, and may even diverge if M_T is such that we have $v_t = 0$. It is true that when $v_t = 0$ we have unnatural, complete cancellation, but in our work we only use v_t in a binary way: to distinguish cases with viable ΔT from those with unacceptably large ΔT. Once v_t is small enough to have viable ΔT, we do not care whether $v_t = 1$ GeV or $v_t = 0.01$ GeV, for example.

As in Sec. II, we can also estimate the fine-tuning in ΔT due to M_T as shown in Athron *et al.* [50] when there is a cancellation in the numerator of Eq. (36) that makes ΔT small. With all parameters other than M_T fixed, we first compute M_T^* such that for $M_T > M_T^*$, ΔT is always viable ($\Delta T < 0.1$), and define fine-tuning as

$$\kappa' \equiv \frac{M_T^*}{\text{Range of } M_T (\text{with } M_T < M_T^*) \text{ that gives viable } \Delta T}. \quad (80)$$

This definition of fine-tuning is harder to implement because, given a set of parameters except M_T, we first have to find out if regions of M_T allowed by ΔT comes about because of cancellations, before we can apply Eq. (80). For example, it is possible that ΔT is always viable for any value of M_T (as are the cases for Points 3 through 6 of Table I), so that we can not apply Eq. (80) as there is no fine-tuning in ΔT. Despite its limited applicability compared to κ_T, κ_T' may be a more reasonable measure of fine-tuning when there is a cancellation that leads to a small value for ΔT. For Point 1(2) in Table I, we have $\kappa_T \sim 33(11)$ and $\kappa_T' \sim 4.7(6.4)$, corresponding to a 33(11)% change in ΔT per a 1% change in M_T, and also cancellation of one part in 4.7(6.4). For the other four points in Table I where κ_T' in Eq. (80) is not well defined, the values of κ_T are small, indicating small fine-tuning for these sets of parameters. Since a complete analysis of fine-tuning in the triplet sector in the TESSM is outside the scope of this work, we will conclude this section noting that in an extreme case [Eq. (37)], $\kappa_T' \sim 24$, so we suspect that the typical fine-tuning in the triplet sector be less than one part in 24.

V. CONCLUSIONS

In this work, we have revisited a very simple extension to the MSSM by adding a hypercharge-neutral, $SU(2)$-triplet chiral superfield. We considered this model as a reasonably economical extension of the MSSM and an alternative to the NMSSM, and extended the phenomenological studies in several directions. In addition to discussing the decoupling behavior of the triplets and comparing it to the decoupling behavior of the singlet of the NMSSM, we have computed the mass of the lightest CP-even Higgs boson to one loop in the large quartic coupling λ. With λ, the Higgs-triplet-Higgs coupling in the superpotential, being comparable with the top Yukawa coupling, we find that the model is able to satisfy LEP2 bounds on the Higgs mass without contributions from the s-top sector. At the expense of perturbativity at the GUT scale, we have checked that the model can give much smaller fine-tuning in the electroweak sector than the MSSM. In the triplet sector, there may be fine-tuning in having small oblique corrections, but we estimate this fine-tuning to be no worse than about one part in 30.

With large λ, the TESSM opens up previously forbidden regions of parameters in the MSSM. In particular, both s-tops can be light in the TESSM. The light s-tops can then lead to phenomenology that is very different from the MSSM with important implications for the LHC, such as a Higgs boson that is both gluophilic and photophobic.

Our simple analysis here can be extended in many directions, and these further studies must be done if the model is going to make precise predictions at the LHC. With large λ, there can be important higher-loop effects to the mass of the lightest, CP-even Higgs boson. Furthermore, important higher-loop QCD effects must also be included to properly study the gluon-gluon fusion production and the diphoton decay of the Higgs boson. We leave these open projects for the future and hope they may add to the already rich possibilities of phenomenology that will be seen at the LHC.

ACKNOWLEDGMENTS

This work is supported by the U.S. National Science Foundation under Grants No. PHY-0354226, No. PHY-

0555545, and No. PHY-0354838. We are indebted to R. Sekhar Chivukula and Elizabeth S. Simmons for inspiring this project and many useful discussions. We would also like to thank Neil D. Christensen and Puneet Batra for helpful comments and suggestions. The Feynman diagrams in this work are drawn using JAXODRAW [59], and we check some of our results using HDECAY [60].

APPENDIX A: FIELD-DEPENDENT MASS MATRICES

In this appendix, we list the field-dependent matrices that enter into the Coleman-Weinberg potential in Eq. (55). We have five mass matrices, one for each set of particles: the CP-even Higgs bosons ($\mathcal{M}_a$), the CP-odd Higgs bosons ($\mathcal{M}_b$), the charged Higgs bosons ($\mathcal{M}_c$), the neutralinos ($\mathcal{M}_{\tilde{N}}$), and the charginos ($\mathcal{M}_{\tilde{C}}$). We first list the elements of the Higgs bosons.

$$(\mathcal{M}_a^2)_{11} = m_{H_u}^2 + \mu^2 + \frac{1}{8}(g_1^2 + g_2^2)(3a_u^2 - a_d^2) + \frac{\lambda^2}{2}(a_t^2 + a_d^2) - \sqrt{2}\lambda\mu a_t, \tag{A1}$$

$$(\mathcal{M}_a^2)_{12} = -B_\mu - \frac{1}{4}(g_1^2 + g_2^2)a_u a_d + \lambda^2 a_u a_d + \frac{\lambda}{\sqrt{2}}(A_\lambda + M_T)a_t, \tag{A2}$$

$$(\mathcal{M}_a^2)_{13} = \lambda^2 a_u a_t - \sqrt{2}\lambda\mu a_u + \frac{\lambda}{\sqrt{2}}(A_\lambda + M_T)a_d, \tag{A3}$$

$$(\mathcal{M}_a^2)_{22} = m_{H_d}^2 + \mu^2 + \frac{\lambda^2}{2}(a_t^2 + a_u^2) + \frac{1}{8}(g_1^2 + g_2^2)(3a_d^2 - a_u^2) - \sqrt{2}\lambda\mu a_t, \tag{A4}$$

$$(\mathcal{M}_a^2)_{23} = \lambda^2 a_d a_t - \sqrt{2}\lambda\mu a_d + \frac{\lambda}{\sqrt{2}}(A_\lambda + M_T)a_u, \tag{A5}$$

$$(\mathcal{M}_a^2)_{33} = M_T^2 + m_T^2 + B_T + \frac{\lambda^2}{2}(a_d^2 + a_u^2), \tag{A6}$$

$$(\mathcal{M}_b^2)_{11} = m_{H_u}^2 + \mu^2 + \frac{1}{8}(g_1^2 + g_2^2)(a_u^2 - a_d^2) + \frac{\lambda^2}{2}(a_t^2 + a_d^2) - \sqrt{2}\lambda\mu a_t, \tag{A7}$$

$$(\mathcal{M}_b^2)_{12} = B_\mu - \frac{\lambda}{\sqrt{2}}(M_T + A_\lambda)a_t, \tag{A8}$$

$$(\mathcal{M}_b^2)_{13} = \frac{\lambda}{\sqrt{2}}(M_T - A_\lambda)a_d, \tag{A9}$$

$$(\mathcal{M}_b^2)_{22} = m_{H_d}^2 + \mu^2 + \frac{1}{8}(a_d^2 - a_u^2)(g_1^2 + g_2^2) + \frac{\lambda^2}{2}(a_t^2 + a_u^2) - \sqrt{2}\lambda\mu a_t, \tag{A10}$$

$$(\mathcal{M}_b^2)_{23} = \frac{\lambda}{\sqrt{2}}(M_T - A_\lambda)a_u, \tag{A11}$$

$$(\mathcal{M}_b^2)_{33} = M_T^2 + m_T^2 - B_T + \frac{\lambda^2}{2}(a_d^2 + a_u^2), \tag{A12}$$

$$(\mathcal{M}_c^2)_{11} = m_{H_u}^2 + \mu^2 + \left(\lambda^2 - \frac{g_1^2 - g_2^2}{8}\right)a_d^2 + \frac{1}{8}(g_1^2 + g_2^2)a_u^2 + \sqrt{2}\lambda\mu a_t + \frac{\lambda^2}{2}a_t^2, \tag{A13}$$

$$(\mathcal{M}_c^2)_{12} = B_\mu + \frac{1}{2}\left(\lambda^2 + \frac{g_2^2}{2}\right)a_d a_u + \frac{\lambda}{\sqrt{2}}(M_T + A_\lambda)a_t, \tag{A14}$$

$$(\mathcal{M}_c^2)_{13} = \lambda\mu a_u + \frac{1}{\sqrt{2}}\left(\lambda^2 - \frac{g_2^2}{2}\right)a_u a_t - \lambda M_T a_d, \tag{A15}$$

$$(\mathcal{M}_c^2)_{14} = \lambda\mu a_u - \frac{1}{\sqrt{2}}\left(\lambda^2 - \frac{g_2^2}{2}\right)a_u a_t - \lambda A_\lambda a_d, \tag{A16}$$

$$(\mathcal{M}_c^2)_{22} = m_{H_d}^2 + \mu^2 + \left(\lambda^2 - \frac{g_1^2 - g_2^2}{8}\right)a_u^2 + \frac{1}{8}(g_1^2 + g_2^2)a_d^2 + \sqrt{2}\lambda\mu a_t + \frac{\lambda^2}{2}a_t^2, \tag{A17}$$

$$(\mathcal{M}_c^2)_{23} = -\lambda\mu a_d + \frac{1}{\sqrt{2}}\left(\lambda^2 - \frac{g_2^2}{2}\right)a_d a_t + \lambda A_\lambda a_u, \tag{A18}$$

$$(\mathcal{M}_c^2)_{24} = -\lambda\mu a_d - \frac{1}{\sqrt{2}}\left(\lambda^2 - \frac{g_2^2}{2}\right)a_d a_t + \lambda M_T a_u, \tag{A19}$$

$$(\mathcal{M}_c^2)_{33} = M_T^2 + m_T^2 + \frac{g_2^2}{4}(a_d^2 + 2a_t^2 - a_u^2) + \lambda^2 a_u^2, \tag{A20}$$

$$(\mathcal{M}_c^2)_{34} = B_T - \frac{g_2^2}{2}a_t^2, \tag{A21}$$

$$(\mathcal{M}_c^2)_{44} = M_T^2 + m_T^2 + \frac{g_2^2}{4}(a_u^2 + 2a_t^2 - a_d^2) + \lambda^2 a_d^2, \tag{A22}$$

where $m_{H_{u,d}}^2$ satisfy the minimization conditions Eqs. (28) and (29).

For the neutralino and charginos, since we do not take into account mixing with the gauginos, we have reduced matrices compared to those in Eqs. (40) and (42), and here we can simply replace the vevs by the corresponding particle

$$\mathcal{M}_{\tilde{N}} = \begin{pmatrix} 0 & -\mu + \frac{\lambda}{\sqrt{2}} a_t & \frac{1}{\sqrt{2}} \lambda a_u \\ -\mu + \frac{\lambda}{\sqrt{2}} a_t & 0 & \frac{1}{\sqrt{2}} \lambda a_d \\ \frac{1}{\sqrt{2}} \lambda a_u & \frac{1}{\sqrt{2}} \lambda a_d & M_T \end{pmatrix}, \quad \text{(A23)}$$

$$\mathcal{M}_{\tilde{C}} = \begin{pmatrix} \mu + \frac{\lambda}{\sqrt{2}} a_t & -\lambda a_d \\ \lambda a_u & M_T \end{pmatrix}. \quad \text{(A24)}$$

APPENDIX B: DIPHOTON DECAY WIDTH OF A REAL SCALAR

In this appendix, we review the formula for the decay width of a real scalar ϕ^0 (with mass m_ϕ) decaying into two photons $\Gamma(\phi^0 \to \gamma\gamma)$ [52]. Generally, given the interactions

$$\mathcal{L} \supset -A_s s^+ s^- \phi^0 - \frac{A_\psi}{2} \phi^0 \bar{\psi}\psi + A_W W^{+\mu} W^-_\mu \phi^0, \quad \text{(B1)}$$

where $s^\pm$ (ψ) $\{W^\pm_\mu\}$ is a charged scalar (fermion) {gauge boson} with mass m_s (m_ψ) $\{m_W\}$ and electric charge Q_s (Q_ψ) $\{Q_W\}$, the diphoton partial decay width is given by

$$\Gamma(\phi^0 \to \gamma\gamma) = \frac{\alpha^2_{\rm em}}{1024\pi^3} m_\phi \left| N_\psi A_\psi Q^2_\psi \frac{m_\phi}{m_\psi} F_\psi + N_s A_s Q^2_s \frac{m_\phi}{m^2_s} F_s + N_W A_W Q^2_W \frac{m_\phi}{m^2_W} F_W \right|^2, \quad \text{(B2)}$$

where N_i are factors to account for additional degrees of freedom (such as color) and

$$F_s = \tau_s[1 - \tau_s f(\tau_s)], \quad \text{(B3)}$$

$$F_\psi = -2\tau_\psi[1 + (1 - \tau_\psi) f(\tau_\psi)], \quad \text{(B4)}$$

$$F_W = 2 + 3\tau_W + 3\tau_W(2 - \tau_W) f(\tau_W), \quad \text{(B5)}$$

where

$$\tau_i \equiv 4\frac{m^2_i}{m^2_\phi}, \quad \text{for } i = s, \psi, W, \quad \text{(B6)}$$

$$f(\tau) = \begin{cases} (\arcsin\sqrt{\frac{1}{\tau}})^2 & \text{if } \tau > 1, \\ -\frac{1}{4}(\ln\frac{\eta_+}{\eta_-} - i\pi)^2 & \text{if } \tau < 1, \end{cases} \quad \text{(B7)}$$

$$\eta_\pm \equiv 1 \pm \sqrt{1 - \tau}. \quad \text{(B8)}$$

In the case of colored particles, we can make the replacement

$$N Q^4 \alpha^2_{\rm em} \to 2\alpha^2_s \quad \text{(B9)}$$

to compute the digluon decay width $\Gamma(\phi^0 \to gg)$, which is related to the gluon-gluon fusion production cross section by

$$\sigma(gg \to \phi^0) = \frac{\pi^2}{8m^3_\phi} \Gamma(\phi^0 \to gg). \quad \text{(B10)}$$

[1] M. Drees, arXiv:hep-ph/9611409.
[2] S. P. Martin, arXiv:hep-ph/9709356.
[3] M. Dine, arXiv:hep-ph/9612389.
[4] M. E. Peskin, arXiv:0801.1928.
[5] M. Acciarri *et al.* (L3 Collaboration), Phys. Lett. B **519**, 33 (2001).
[6] A. Heister *et al.* (ALEPH Collaboration), Phys. Lett. B **526**, 191 (2002).
[7] G. Abbiendi *et al.* (OPAL Collaboration), Eur. Phys. J. C **26**, 479 (2003).
[8] J. Abdallah *et al.* (DELPHI Collaboration), Eur. Phys. J. C **32**, 145 (2004).
[9] R. Barate *et al.* (LEP Working Group for Higgs Boson Searches and ALEPH Collaboration), Phys. Lett. B **565**, 61 (2003).
[10] Y. Okada, M. Yamaguchi, and T. Yanagida, Prog. Theor. Phys. **85**, 1 (1991).
[11] H. E. Haber and R. Hempfling, Phys. Rev. Lett. **66**, 1815 (1991).
[12] H. E. Haber and R. Hempfling, Phys. Rev. D **48**, 4280 (1993).
[13] H. E. Haber, R. Hempfling, and A. H. Hoang, Z. Phys. C **75**, 539 (1997).
[14] S. Heinemeyer, W. Hollik, and G. Weiglein, Phys. Lett. B **440**, 296 (1998).
[15] S. Heinemeyer, W. Hollik, and G. Weiglein, Phys. Lett. B **455**, 179 (1999).
[16] S. Heinemeyer, W. Hollik, and G. Weiglein, J. High Energy Phys. 06 (2000) 009.
[17] J. R. Espinosa and R. J. Zhang, J. High Energy Phys. 03 (2000) 026.
[18] M. S. Carena, H. E. Haber, S. Heinemeyer, W. Hollik, C. E. M. Wagner, and G. Weiglein, Nucl. Phys. **B580**, 29 (2000).

[19] J. R. Espinosa and R. J. Zhang, Nucl. Phys. **B586**, 3 (2000).
[20] M. Bastero-Gil, C. Hugonie, S. F. King, D. P. Roy, and S. Vempati, Phys. Lett. B **489**, 359 (2000).
[21] C. Balazs, M. S. Carena, A. Freitas, and C. E. M. Wagner, J. High Energy Phys. 06 (2007) 066.
[22] P. N. Pandita, Z. Phys. C **59**, 575 (1993).
[23] P. N. Pandita, Phys. Lett. B **318**, 338 (1993).
[24] T. Elliott, S. F. King, and P. L. White, Phys. Rev. D **49**, 2435 (1994).
[25] S. Codoban and M. Jurcisin, Acta Phys. Slovaca **52**, 253 (2002).
[26] D. J. Miller, R. Nevzorov, and P. M. Zerwas, Nucl. Phys. **B681**, 3 (2004).
[27] U. Ellwanger and C. Hugonie, Phys. Lett. B **623**, 93 (2005).
[28] U. Ellwanger and C. Hugonie, Mod. Phys. Lett. A **22**, 1581 (2007).
[29] J. R. Espinosa and M. Quiros, Nucl. Phys. **B384**, 113 (1992).
[30] J. R. Espinosa and M. Quiros, Phys. Lett. B **279**, 92 (1992).
[31] O. Felix-Beltran, Int. J. Mod. Phys. A **17**, 465 (2002).
[32] N. Setzer and S. Spinner, Phys. Rev. D **75**, 117701 (2007).
[33] J. L. Diaz-Cruz, J. Hernandez-Sanchez, S. Moretti, and A. Rosado, Phys. Rev. D **77**, 035007 (2008).
[34] R. Sekhar Chivukula, N. D. Christensen, and E. H. Simmons, Phys. Rev. D **77**, 035001 (2008).
[35] R. N. Mohapatra and G. Senjanovic, Phys. Rev. D **23**, 165 (1981).
[36] R. N. Mohapatra, N. Okada, and H. B. Yu, Phys. Rev. D **77**, 115017 (2008).
[37] R. N. Mohapatra, N. Setzer, and S. Spinner, J. High Energy Phys. 04 (2008) 091.
[38] T. Blank and W. Hollik, Nucl. Phys. **B514**, 113 (1998).
[39] M. C. Chen, S. Dawson, and T. Krupovnickas, Int. J. Mod. Phys. A **21**, 4045 (2006).
[40] M. C. Chen, S. Dawson, and T. Krupovnickas, Phys. Rev. D **74**, 035001 (2006).
[41] P. H. Chankowski, S. Pokorski, and J. Wagner, Eur. Phys. J. C **50**, 919 (2007).
[42] P. H. Chankowski and J. Wagner, Phys. Rev. D **77**, 025033 (2008).
[43] K. S. Babu, X. G. He, and S. Pakvasa, Phys. Rev. D **33**, 763 (1986).
[44] S. Willenbrock, Phys. Lett. B **561**, 130 (2003).
[45] J. Sayre, S. Wiesenfeldt, and S. Willenbrock, Phys. Rev. D **73**, 035013 (2006).
[46] P. Batra, A. Delgado, D. E. Kaplan, and T. M. P. Tait, J. High Energy Phys. 02 (2004) 043.
[47] R. Harnik, G. D. Kribs, D. T. Larson, and H. Murayama, Phys. Rev. D **70**, 015002 (2004).
[48] S. Chang, C. Kilic, and R. Mahbubani, Phys. Rev. D **71**, 015003 (2005).
[49] A. Delgado and T. M. P. Tait, J. High Energy Phys. 07 (2005) 023.
[50] P. Athron and D. J. Miller, Phys. Rev. D **76**, 075010 (2007).
[51] S. R. Coleman and E. Weinberg, Phys. Rev. D **7**, 1888 (1973).
[52] J. F. Gunion and H. E. Haber, Nucl. Phys. **B272**, 1 (1986); **B402**, 567(E) (1993).
[53] S. Dawson, A. Djouadi, and M. Spira, Phys. Rev. Lett. **77**, 16 (1996).
[54] R. V. Harlander and M. Steinhauser, J. High Energy Phys. 09 (2004) 066.
[55] W. M. Yao *et al.* (Particle Data Group), J. Phys. G **33**, 1 (2006).
[56] R. Barbieri and G. F. Giudice, Nucl. Phys. **B306**, 63 (1988).
[57] G. W. Anderson and D. J. Castano, Phys. Lett. B **347**, 300 (1995).
[58] G. W. Anderson and D. J. Castano, Phys. Rev. D **52**, 1693 (1995).
[59] D. Binosi and L. Theussl, Comput. Phys. Commun. **161**, 76 (2004).
[60] A. Djouadi, J. Kalinowski, and M. Spira, Comput. Phys. Commun. **108**, 56 (1998).